Electric Power Systems Research 211 (2022) 108191

Contents lists available at ScienceDirect

Electric Power Systems Research

journal homepage: www.elsevier.com/locate/epsr

Frequency control studies: A review of power system, conventional and renewable generation unit modeling

Ana Fernández-Guillamón [a], Eduard Muljadi [b], Angel Molina-García [c,*]

[a] Department of Electrical, Electronics and Automatics Engineering, and Applied Physics, Universidad Politécnica de Madrid, 28012 Madrid, Spain
[b] Department of Electrical and Computer Engineering, Auburn University, 220 Broun Hall, Auburn, AL 36849, USA
[c] Department of Automatics, Electrical Eng. and Electronic Tech., Universidad Politécnica de Cartagena, 30202 Cartagena, Spain

ARTICLE INFO

Keywords:
Power system stability
Frequency control
Power system modeling
Conventional power plants
Renewable energy sources

ABSTRACT

Over the last decades, renewable energy sources have increased considerably their generation share in power systems. As a consequence, in terms of frequency deviations, both grid reliability and stability have raised interest. By considering the absence of a consensual set of models for frequency control analysis, both for the different generation units (conventional and renewables) and the power system itself, this paper provides extensive and significant information focused on the models and parameters for studies about frequency control and grid stability. An extensive analysis of supply-side and power system modeling for frequency stability studies over the last decade is presented and reviewed. Parameters commonly used and assumed in the specific literature for such simulations are also given and compared. Modeling of generation units are described as well, including both conventional and renewable power plants.

1. Introduction

Frequency is a crucial parameter in power systems. Imbalances between supply and demand cause deviations from the nominal frequency: a supply-side excess yields an increase in frequency, while a demand-side excess results in a decrease in frequency [1]. Under large grid frequency deviations, statutory and operational limits can be breached, forcing generators to disconnect and resulting in catastrophic failures within the system [2]. With the increasing integration of renewable sources into power systems, it is expected that frequency events severity becomes more and more important as conventional units are supplanted by renewable generators [3]. In fact, and apart from the intermittent nature of renewables, most of these renewable resources are decoupled from the grid. Consequently, they do not contribute to the system inertia, commonly considered as one of the crucial grid parameters to ensure a synchronized operation of current power systems [4]. Indeed, according to Dreidy et al. [5], an inertia reduction of 70% is expected between 2014–2034 as a result of the renewable integration, thus needing a more 'flexible' power system [6]. Table 1 compares dispatchable generation units in terms of flexibility dimensions: `Min. generation` refers to the minimum stable output power that a power plant can achieve, expressed as a percentage of their nominal output capacity; `Ramp rate` represents the maximum power per minute a power plant can increase or decrease its generation (in percentage of the nominal output capacity); and `Start-up time` corresponds to the start-up of the power plant from warm conditions (i.e., 8 to 60 h of shutdown) [7]. As can be seen, these power plants show relevant differences in their technical flexibility, which should be considered for future high renewable energy source integration into power systems [8].

Table 1
Conventional power plant characteristics according to [7].

Power plant	Min. generation (%)	Ramp rate (%/min)	Start-up time (h)
Steam turbine (gas/oil)	30–60	2–8	3–8
Nuclear	90	2	24
CCGT	40	8	3
Hydro	0–50	5–15	0.16
Bioenergy	50	8	3

In the specific literature, there are many studies focused on frequency control, power system stability, and imbalance scenarios. Fig. 1 depicts the main elements usually considered in such studies. Due to the increased penetration of renewables in current electrical grids, different authors have proposed and assessed inertial response capability from them during the last decade [9,10], mainly wind power plants [11,12] and PV installations [13,14]. However, these contributions usually evaluate power systems' stability through different power systems and

* Corresponding author.
E-mail address: angel.molina@upct.es (A. Molina-García).

https://doi.org/10.1016/j.epsr.2022.108191
Received 31 January 2022; Received in revised form 26 April 2022; Accepted 12 June 2022
Available online 2 July 2022

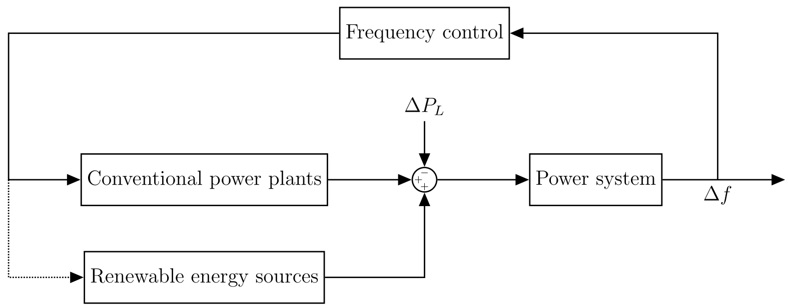

Fig. 1. General overview.

generation units' models, together with different scenarios and power imbalances, thus making it difficult to compare the results of the frequency control strategies proposed in different studies. In addition, a variety of models for the same generation units are usually considered by the authors.

Under this framework, this paper describes and compares power system and generation units' modeling for frequency control analysis based on an extensive literature review for the last decade, including the parameters commonly used in previous contributions – both for conventional and renewable generation unit modeling –. The specific frequency control strategies are not included, as several reviews focused on both conventional and renewable energy sources are available in the specific literature [5,15–20]. Most of the models presented in this paper are linear (based on transfer functions) to obtain time-domain responses. Subsequently, these models are suitable to analyze the system behavior under small-signal stability [21], even though current studies also use such models to analyze the loss of the largest power plant, providing proper results [22–24]. Consequently, and despite the models can be used to simulate severe power imbalances, they are not robust enough to variations in the operating conditions. Moreover, it should be noticed that these models should be used for qualitative studies, and may lack the precision needed by Transmission System Operators (TSO) [25], who can perform a fully nonlinear simulation of the power system behavior.

The rest of the paper is structured as follows. Section 2 provides the models and parameters most commonly adopted for the power systems modeling focused on frequency stability analysis. In Section 3, the models and parameters of conventional power plants are discussed. Models and parameters about renewable sources are presented in Section 4. Section 5 compares the different values for the parameters, to understand how them affect the simulation results. Section 6 presents the discussion. Finally, conclusions are given in Section 7.

2. Power system modeling for frequency analysis

According to the specific literature, most frequency oscillation studies propose an equivalent power system model by considering the swing equation, in which all grid synchronous generators are summarized in an equivalent rotating mass, with an equivalent inertia constant H_{eq} [26]. This H_{eq} is estimated with:

$$H_{eq} = \frac{\sum_{i=1}^{SG} H_i \cdot S_{B,i}}{S_B}, \tag{1}$$

where H_i and $S_{B,i}$ are the inertia constant and rated power of the synchronous generator i (respectively), SG is the total number of synchronous generators connected to the grid, and S_B is the rated power of the power system [21]. Hence, the swing equation of the power system is [27–42]:

$$\Delta f = \frac{1}{(2 \cdot H_{eq}) \cdot s + D} \cdot (\Delta P_g - \Delta P_L), \tag{2}$$

where H_{eq} [s] is the equivalent inertia of the grid, and D [W/Hz] is the damping factor, which models the dependency of loads power to frequency [43], even though there are more "damping elements" in a power system (i.e., speed governing, excitation system, etc.) [44]. Other authors replace $2 \cdot H_{eq}$ by M [s] [45–54], and other contributions propose and use the following expression [55–64],

$$\Delta f = \frac{K_P}{T_P \cdot s + 1} \cdot (\Delta P_g - \Delta P_L), \tag{3}$$

being $K_p = 1/D$ [Hz/W] and $T_P = 2 \cdot H_{eq}/D$ [W^{-1}]. Consequently, regardless of the equation used, both H_{eq} and D are crucial parameters for the power system stability, as both reduce the impact of power variations in frequency [3]. The models corresponding to Eqs. (2) and (3) are shown in Fig. 2. Tables 2 and 3 summarize values found in the literature for H_{eq} and D sorted in chronological order, also including the H_{eq} values of those studies where $H_{eq} = M/2$. From the information given in Table 2, a wider range of inertia values can be even found in [34], which suggested H_{eq}=21.08 s for grid-connected mode in line with micro-grid model parameters used in [65,66]. Tables 4 and 5 give the values for K_P and T_P respectively, as well as the values for D and H_{eq} determined from:

$$D = \frac{1}{K_P}, \tag{4}$$

$$H_{eq} = \frac{T_P \cdot D}{2}. \tag{5}$$

As can be seen, there are severe differences among the values considered in each study to simulate the equivalent power system model, which affect considerably the corresponding frequency excursions in terms of nadir and rate of change of frequency (RoCoF) [67]. In fact, there is a relevant heterogeneity regarding equivalent power system inertia values, which can be derived from the different synchronous power plants connected to the grid in each study – refer to Eq. (1) –. This may be caused by the important differences existing among the inertia constant of power plants, mainly depending on their type and rated power as detailed in [19]. With regard to the damping factor, remarkable differences are found in the specific literature as well. Furthermore, it is crucial to estimate an accurate value of D for power systems under disturbances, as this parameter highly influences the results and, subsequently, can have a relevant impact on the study [68]. Frequency control of power systems for stability analysis are also sensitive to such parameter values. Moreover, virtual damping and virtual inertia based on the small-signal stability are currently topics of interest for the scientific community [69,70]. Nevertheless, such topics are out of the aim of this paper and they have been extensively discussed in other contributions [71–75].

3. Supply-side: Conventional thermal power plant modeling

In frequency stability studies, thermal power plants have been traditionally and still typically used by TSO for frequency control purposes [82]. As a usual term, thermal power plants mainly refer to those based on fossil fuels: coal, oil, and natural gas [83], which still represent an important share in current power systems. For instance, coal-fired power plants fueled 38% of global electricity in 2020 [84].

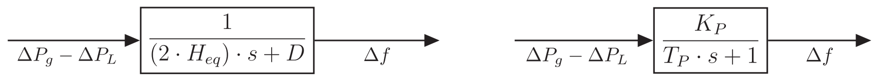

(a) Eq. (2) (b) Eq. (3)

Fig. 2. Power system models for frequency stability studies simulations.

Table 2
Values of equivalent inertia constant (H_{eq}) for frequency analysis.

Constant	Value	Refs.	Year
H_{eq}	5	[76]	2004
H_{eq}	4–5	[28]	2010
H_{eq}	3.5	[77]	2012
H_{eq}	4–5	[29]	2012
H_{eq}	5	[78]	2013
H_{eq}	5–6	[45]	2013
H_{eq}	5–6	[51]	2017
H_{eq}	5	[60]	2017
H_{eq}	7.11	[34]	2017
H_{eq}	5	[79]	2017
H_{eq}	5–6	[36]	2017
H_{eq}	5	[37]	2017
H_{eq}	5	[42]	2019
H_{eq}	3–3.3	[80]	2020
H_{eq}	4	[81]	2020

Table 3
Values of equivalent damping factor (D) for frequency analysis.

Constant	Value	Refs.	Year
D	0.8	[76]	2004
D	0.6–0.9	[28]	2010
D	0.1	[30]	2012
D	0.6–0.9	[29]	2012
D	0.01	[78]	2013
D	0.0084–1.8	[45]	2013
D	1.5	[51]	2017
D	1–3	[37]	2017
D	0.01	[60]	2017
D	1–1.8	[36]	2017
D	0.8–1	[42]	2019

Table 4
Values of K_P and D ($1/K_P$) for frequency analysis.

Constant	Value	Constant	Value	Refs.	Year
K_P	120	D	0.0083	[55]	2012
K_P	115–120	D	0.0087–0.0083	[58]	2016
K_P	120	D	0.0083	[59]	2016
K_P	20–120	D	0.05–0.0083	[63]	2019
K_P	120	D	0.0083	[64]	2019

Table 5
Values of T_P and H_{eq} ($T_P \cdot D/2$) for frequency analysis.

Constant	Value	Constant	Value	Refs.	Year
T_P	10	H_{eq}	0.0417	[55]	2012
T_P	10–20	H_{eq}	0.0435–0.083	[58]	2016
T_P	20	H_{eq}	0.083	[59]	2016
T_P	3.76–20	H_{eq}	0.094–0.083	[63]	2019
T_P	20	H_{eq}	0.083	[64]	2019

3.1. Steam turbines

With regard to steam turbines, they have different turbine dimensions depending on the cycle pressures; i.e., high pressure, intermediate pressure, and low pressure. In current thermal power plants, the steam from the high pressure turbine goes back to the power plant to be reheated. It goes through the intermediate pressure turbine, and then it is conducted to the low pressure turbine by means of the cross-over pipe. The efficiency of the thermodynamic cycle is increased by reheating the steam [85]. In the literature review, steam turbines for frequency analysis are usually modeled by two different approaches: non-reheat steam turbines [28,29,35,36,51–54,59,63,64] and single-reheat steam turbines [30,31,38,39,42,55,57–64,81]. Both approaches include the governor, modeled as a first-order transfer function ($1/(1+s\,T_g)$), as summarized in Fig. 3. In these block diagrams, P_{sp} [W] is the set-point power, T_g [s] is the time constant of the governor, T_{CH} [s] is the time constant of the steam chest and the inlet piping, T_{RH} [s] is the time constant of the re-heater, F_{HP} [–] is the fraction of total turbine power generated by the *HP* body of the turbine, and P_g [W] is the generated power. Typical values of these parameters are given in Table 6 for non-reheat steam turbine, and in Table 7 for single-reheat steam turbine.

Table 6
Non-reheat steam turbine: parameters (Fig. 3(a)).

Parameter	Value	Refs.	Year
T_g	0.2–0.3	[28]	2010
T_g	0.2–0.3	[29]	2012
T_g	0.06–0.17	[45]	2013
T_g	0.1–0.4	[51]	2017
T_g	0.1–0.2	[36]	2017
T_g	0.08	[35]	2017
T_g	0.08	[40]	2019
T_g	0.1–0.4	[52]	2019
T_g	0.06–0.08	[54]	2020
T_{CH}	0.5–0.6	[28]	2010
T_{CH}	0.5–0.6	[29]	2012
T_{CH}	0.3–0.4	[45]	2013
T_{CH}	0.17–0.3	[51]	2017
T_{CH}	0.3–0.4	[36]	2017
T_{CH}	0.4	[35]	2017
T_{CH}	0.4	[40]	2019
T_{CH}	0.17–0.3	[52]	2019
T_{CH}	0.3–0.4	[54]	2020

Table 7
Single-reheat steam turbine: parameters (Fig. 3(b)).

Parameter	Value	Refs.	Year
T_g	0.08	[30]	2012
T_g	0.20	[55]	2012
T_g	0.078–0.082	[58]	2016
T_g	0.08	[59]	2016
T_g	0.20	[80]	2020
T_{CH}	0.30	[30]	2012
T_{CH}	0.30	[55]	2012
T_{CH}	0.30–0.70	[58]	2016
T_{CH}	0.30	[59]	2016
T_{CH}	0.30	[80]	2020
T_{RH}	10	[30]	2012
T_{RH}	10	[55]	2012
T_{RH}	4–4.30	[58]	2016
T_{RH}	10	[59]	2016
T_{RH}	7	[80]	2020
F_{HP}	0.50	[30]	2012
F_{HP}	0.33	[55]	2012
F_{HP}	0.31–0.34	[58]	2016
F_{HP}	0.50	[59]	2016
F_{HP}	0.30	[80]	2020

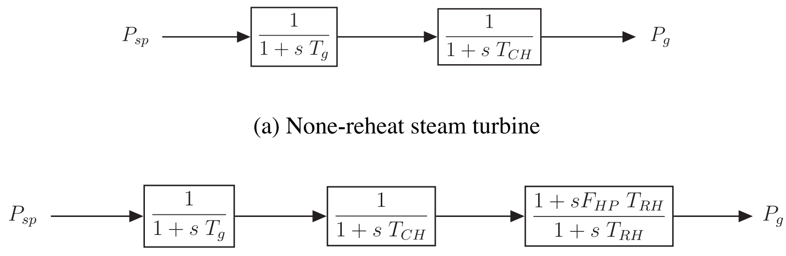

(a) None-reheat steam turbine

(b) Single reheat steam turbine

Fig. 3. Steam turbine models used in frequency control simulations.

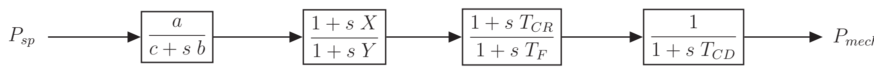

Fig. 4. Gas turbine model.

3.2. Gas turbines

Gas turbines use gas as working fluid, i.e. air, carbon dioxide, or helium [85]. Among the different studies found in the specific literature focused on gas turbines modeling, two main models are identified to give explicitly simulations of such turbines: (*i*) the non-reheat steam turbine modeling depicted in Fig. 3(a) [86,87], being T_g = 0.1 s and T_{CH} = 0.4 s; and (*ii*) the model provided in Fig. 4, by considering a valve positioner, speed governor, fuel system and combustor, and the gas turbine. As can be seen in Fig. 4, a [–] and c [–] are the valve positioner constants, b [s] is the valve positioner time constant, X [s] is the lead time constant of the gas turbine speed governor, Y [s] is the lag time constant of the gas turbine speed governor, T_F [s] is the gas turbine fuel time constant, T_{CR} [s] is the gas turbine combustion reaction time delay, and T_{CD} [s] is the compressor discharge volume time constant [88–90]. These references used the same values for the different parameters: a = 1, b = 0.05 s, c = 1, X = 0.6 s, Y = 1 s, T_F = 0.23 s, T_{CR} = 0.01 s, and T_{CD} = 0.20 s.

3.3. Combined cycle gas turbine

In reference to combined cycle gas turbine (CCGT) plants, it is the result of combining a steam turbine and a gas turbine, each one powering its own generator. As a consequence, a higher efficiency is obtained compared to a conventional thermal plant [85]. CCGT plants are commonly considered for frequency stability studies through the Rowen CCGT model [37,60,61,78,91–93]. Fig. 5 schematically represents such a model. Further information of the parameter values and ranges can be found in [78]. According to Hermans et al. [94], the fast capabilities of CCGT are essential in power systems with high integration of variable Renewable Energy Sources (vRES), as these grids need a more flexible operation, as already detailed in Section 1.

3.4. Nuclear power plants

Due to the high fixed costs and low variable costs of nuclear power plants, and together with security reasons, these generation units usually work as base-load power plants [95,96]. Possible power output variations can then occur under the needs of the plant operator, instead of under the needs of the system operator [97]. Consequently, nuclear power plants do not usually participate in frequency control strategies, subsequently not being considered in most frequency stability studies. In fact, some works which include nuclear power plants in their supply-side, consider its output power as a constant [98–101], thus not modeling the power plant. However, as some national power systems have a large amount of their supply-side from nuclear power plants (e.g., Belgium (50%), Hungary (50%), Ukraine (50%), and France (75%), [102]), advanced nuclear reactors have been currently designed to provide a suitable transient response capability [103]. Moreover, Li *et al.* [104] affirm that, with the increase of the nuclear power share-generation in the world, it is an inexorable trend that nuclear power units will participate in the load-follow operation of future grids.

As nuclear units are based on steam turbines [105], the reheat-steam turbine of Fig. 3(b) can be used as a first approximation to simulate such power plants. However, to the authors' knowledge, no studies focused on load-frequency control included such a model and, consequently, no parameters can be provided. In contrast, based on the model presented in [106], two recent studies provided a linear model to simulate nuclear power plants [107,108], see Fig. 6: T_g [s] is speed governor time constant, T_{T1} [s] is the time constant of LP turbine, T_{RH1} [s] is the time constant of first LP turbine, T_{RH2} [s] is the time constant of second LP turbine; $A = K_{H1} \cdot T_{RH2} + K_{H1} \cdot T_{RH1} + K_{R1} \cdot T_{RH2}$ [s], and $B = K_{H1} \cdot T_{RH1} \cdot T_{RH2}$ [s^2], being K_{H1} [–] the gain of HP turbine, and K_{R1} [–] the gain of the LP turbine. The values used in the simulations for the different parameters were: K_{H1} = 2; K_{R1} = 0.3; T_{T1} = 0.5 s; T_{RH1} = 7 s; T_{RH2} = 9 s.

4. Supply-side: Renewable energy sources modeling

Different and diverse sources are considered as renewable, such as hydropower, wind (onshore and offshore), solar (PV and thermal), biomass, geothermal, and ocean (tide and wave). Among them, hydropower, wind, and PV installations are the most mature technologies to be integrated into power systems [109–111] and their equivalent power plant models are following reviewed in this section.

4.1. Hydro-power plants

Hydro-power plants are commonly modeled and included for frequency analysis in a remarkable amount of works [38,39,42,63,64, 80,81,112–115]. The traditional equivalent modeling of these turbines assumes the following issues [21]: (*i*) the hydraulic resistance is negligible; (*ii*) the penstock pipe is inelastic, being thus incompressible water; (*iii*) water speed varies directly with the gate opening and the square root of the net head; and (*iv*) the turbine output power is proportional to the product of the head and volume flow. Under these premises, the hydro-power turbine transfer function is shown in Fig. 7, being P_{sp} the set-point power, T_g the time constant of the governor, T_R the reset time, R_T the temporary droop, R_P the permanent droop, and T_w the water starting time estimated as follows:

$$T_w = \frac{L \cdot U_0}{a_g \cdot H_0}\,, \tag{6}$$

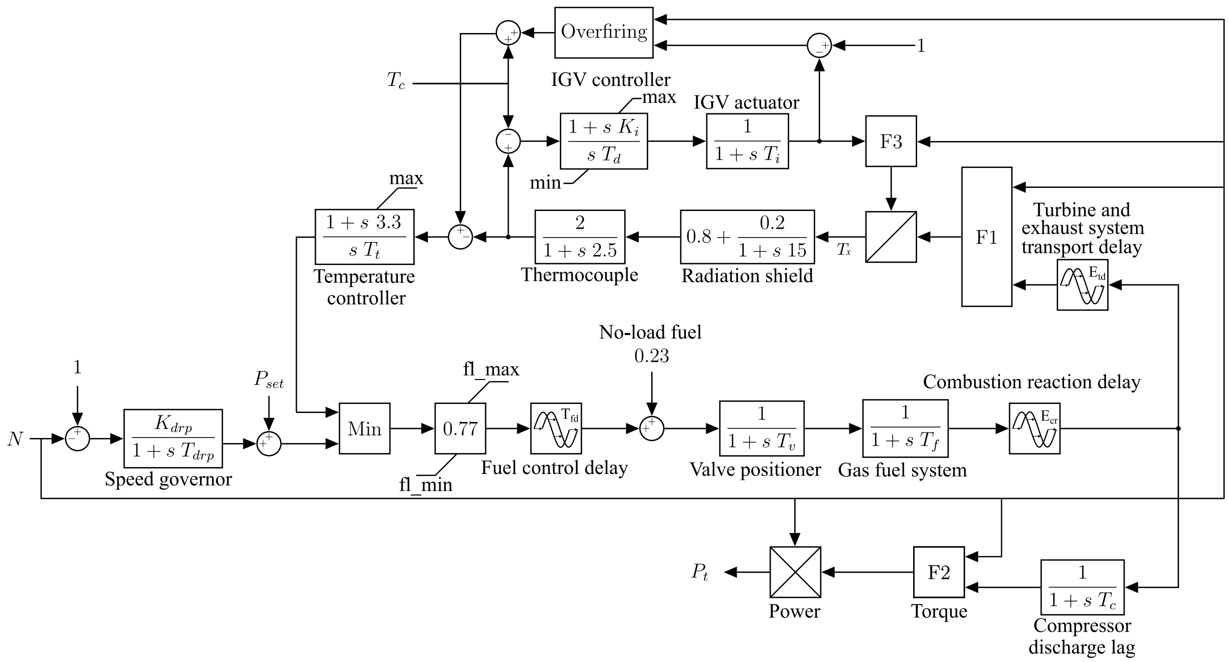

Fig. 5. Rowen CCGT model.

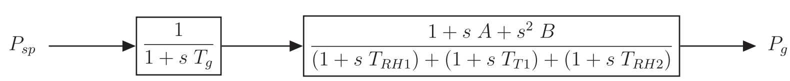

Fig. 6. Linear nuclear power plant model.

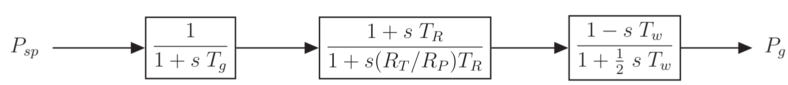

Fig. 7. Classical hydro-power turbine modeling.

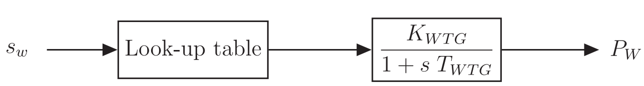

Fig. 8. Simplified equivalent model for a wind turbine.

where H_0 is the initial steady-state of the hydraulic head at gate, U_0 is the initial steady-state of the water velocity, a_g is the constant of gravity and L is the length of conduit. Both R_T and T_R can be determined from:

$$R_T = [2.3 - (T_w - 1) \cdot 0.15] \cdot \frac{T_w}{2 \cdot H}, \tag{7}$$

$$T_R = [5 - (T_w - 1) \cdot 0.5] \cdot T_w, \tag{8}$$

being H the inertia constant of the hydro-power plant [21,116]. Typical values of these parameters are given in Table 8. As can be seen, the same (or quite similar) values are given for the classical hydro-power plant model. Nevertheless, some authors consider that this model is not applicable for hydro-power plants including long penstocks. In such cases, the elasticity of water and conduit should be included and modeled as presented in [117–119]. However, according to Eremia et al. [85], the simplified model of Fig. 7 is suitable for control system studies, such as frequency stability analysis.

Table 8
Hydro-power plant modeling: parameters (see Fig. 7).

Parameters	Value	Refs.	Year
T_w	0.5–4	[21]	1994
T_w	1	[38]	2018
T_w	1	[42]	2019
T_w	1	[63]	2019
T_w	1	[80]	2020
T_R	5	[21]	1994
T_R	5	[38]	2018
T_R	5	[42]	2019
T_R	5	[63]	2019
T_R	5	[80]	2020
R_T	0.38	[21]	1994
R_T	0.38	[38]	2018
R_T	0.38	[80]	2020
R_P	0.05	[21]	1994
R_P	0.05	[38]	2018
R_P	0.05	[80]	2020
T_g	0.2	[21]	1994
T_g	0.2	[38]	2018
T_g	0.6	[63]	2019
T_g	0.2	[42]	2019
T_g	0.2	[80]	2020
R_T/R_P	7.6	[42]	2019
R_T/R_P	6.4	[63]	2019

4.2. Wind power plants

The frequency control based on wind power plants has become an important subject during the last decade [120]. In addition, the wind turbine generator design has an influence on the control mechanism [121,122], being variable wind speed turbine (VWST) the most

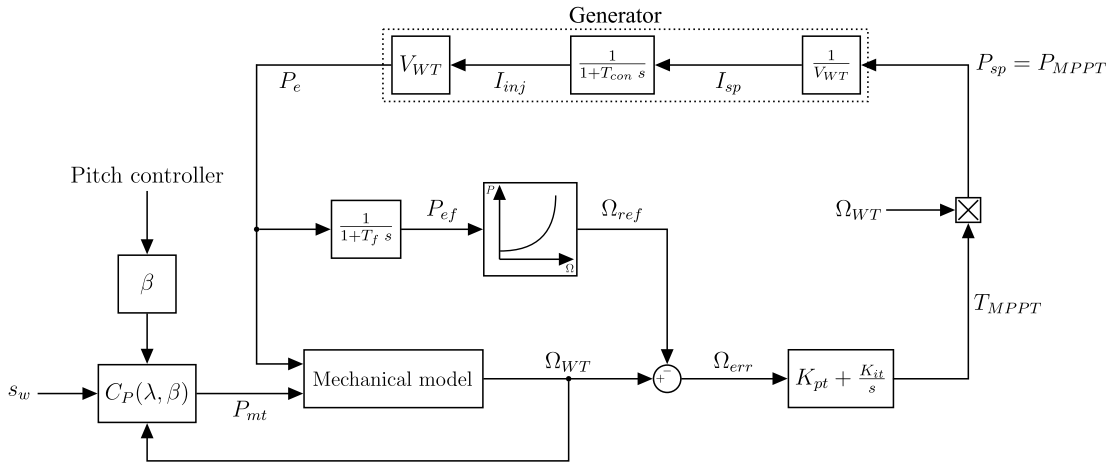

Fig. 9. Equivalent wind turbine model for frequency control strategies.

Table 9
Simple model for wind turbines: parameters (Fig. 8).

Parameters	Value	Refs.	Year
K_{WTG}	1	[79]	2017
K_{WTG}	1	[132]	2018
K_{WTG}	1	[54]	2020
T_{WTG}	1.5 s	[79]	2017
T_{WTG}	0.2 s	[132]	2018
T_{WTG}	1.5 s	[54]	2020

common design and which allows to implement different frequency control strategies or techniques [123–125]. However, these generation units do not sense any grid frequency drop as they are connected to the grid through converters [126], even though wind turbines have similar inertia to conventional generators due to the stored kinetic energy in their rotating masses [127]. Different equivalent wind power plant models have been proposed in the specific literature to provide and evaluate grid frequency stability with high vRES integration [128]. Indeed, some contributions affirm that aggregated and simplified models simulating wind power plants provide similar results for power analysis. In this way, Chang-Chien *et al.* [129] compared wind power plant participation in automatic generation control by (*i*) aggregating individual wind turbines, and (*ii*) assuming a simplified equivalent wind power plant model. Fernández *et al.* [130] modeled wind power plants based on aggregating detailed models of wind turbines, and compared to an equivalent wind turbine for power system dynamic simulations. Conroy *et al.* [131] compared one equivalent wind turbine generator with a re-scaled power capacity to each wind turbine generator modeled separately for transient stability studies.

As a first simplified wind turbine model, different authors have proposed a first-order transfer function [54,79,132] – see Fig. 8 –. Parameters of this model are summarized in Table 9. Nevertheless, the most common model used to simulate an equivalent wind turbine for frequency studies is shown and described in Fig. 9. Regarding the mechanical model, it can either be a one-mass [38–40,115,118,133–138] or two-mass [135,136,138–141] model, see Fig. 10. The two-mass model assumes the rotor and blades as a single mass, and the generator as another mass [23,142,143]. However, most studies analyze frequency deviations with the one-mass mechanical model, assuming it as acceptable due to the consideration of constant voltage [144]. On the contrary, Huerta et al. considers that the two-mass model is the most suitable to evaluate grid stability [145]. In addition to the mechanical model, two main equations estimate the C_p curves from β and λ parameters:

$$C_p(\lambda,\beta) = c_1 \cdot \left(\frac{c_2}{\lambda_i} - c_3\,\beta - c_4\right) e^{\frac{-c_5}{\lambda_i}} + c_6\,\lambda_i. \tag{9}$$

This expression is considered in [33,62,77,81,124,134,140,141,146–149], where c_1 to c_6 values are the wind turbine characteristic coefficients and λ_i is estimated with:

$$\frac{1}{\lambda_i} = \frac{1}{\lambda - 0.08\,\beta} - \frac{0.035}{\beta^3 + 1}. \tag{10}$$

On the other hand, the following expression is taken into account in [23,38,39,46,118,133,150,151]:

$$C_p(\lambda,\beta) = \sum_{i=0}^{4}\sum_{j=0}^{4} \alpha_{i,j} \cdot \beta^i \cdot \lambda^j, \tag{11}$$

being $\alpha_{i,j}$ specific coefficients depending on each specific wind turbine. This expression is proposed in [152,153] to model some General Electric wind turbines for grid studies.

4.3. PV power plants

A PV module is represented by its mathematical characteristic I–V function because of its accuracy and simplicity [154–160]:

$$I_{pv} = N_p \cdot I_{ph} - N_p \cdot I_{rs}\left(e^{\frac{q \cdot V_{MPP}}{k \cdot T \cdot A \cdot N_s}} - 1\right), \tag{12}$$

where N_p is the number of cells in parallel, N_s is the number of cells in series, I_{rs} is the reverse saturation current, q is the electron charge (1.6 $\cdot 10^{-19}$ C), k is the Boltzmann's constant (1.4 $\cdot 10^{-23}$ J/K), A is the ideality factor, T is the temperature, and V_{MPP} is the voltage at maximum power point. I_{ph} is the short-circuit current for one string of the PV panel, which can be estimated with

$$I_{ph} = \left[I_{sc} + K_I (T - T_{ref})\right] \cdot S, \tag{13}$$

being I_{sc} the short-circuit current of the cell, T_{ref} the reference temperature, and K_I the temperature coefficient.

This V_{MPP} for a given irradiation E is calculated based on $V_{MPP,STC}$ (voltage at maximum power point at standard test conditions), which is specified in the data sheet of the PV module. Moreover, V_{MPP} also varies with temperature. A correction factor α_v is thus included. The V_{MPP} is then calculated for any irradiation and temperature with:

$$V_{MPP} = V_{MPP,STC} \cdot \left(\frac{\ln(E)}{\ln(1000)}\right) \cdot [1 + \alpha_v\,(T - T_{STC})]. \tag{14}$$

By multiplying I_{pv} by V_{MPP} (results of Eq. (12) and (14)), the power of the PV module is obtained. In most studies, the PV system is simply modeled by a first-order transfer function to analyze the frequency stability of the power system [161], neglecting any dynamic behavior of the PV power conversion systems [162–166] (see Fig. 11).

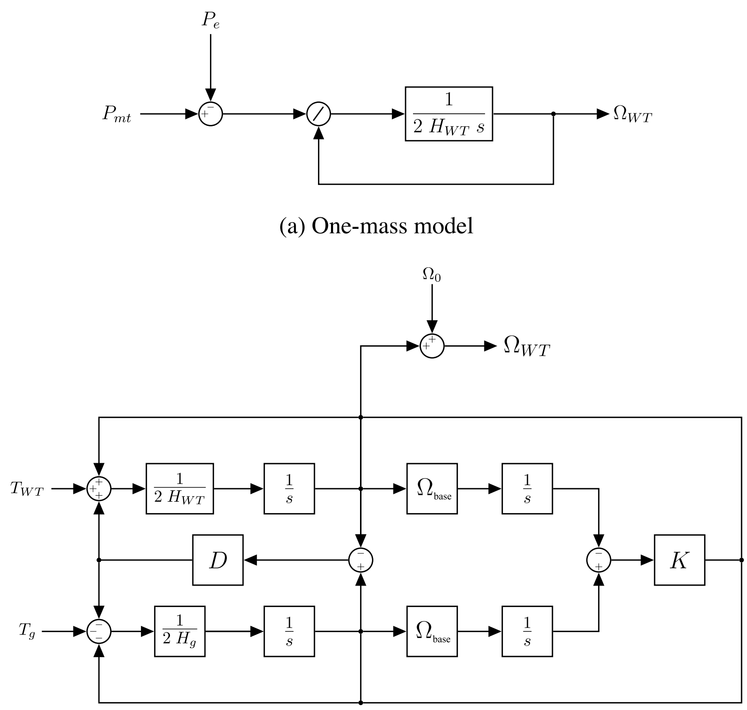

(a) One-mass model

(b) Two-mass model

Fig. 10. Mechanical models for VSWTs.

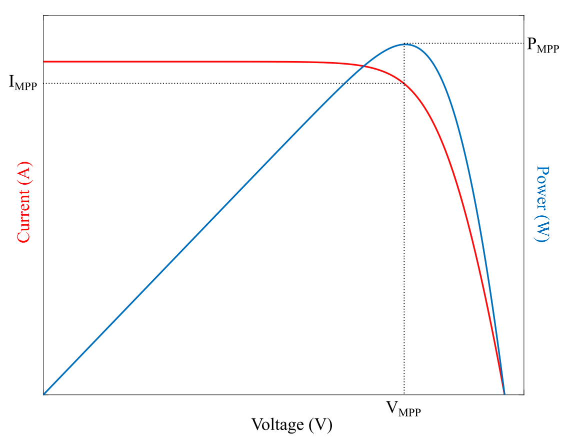

Fig. 11. I-V and P-V curves of a PV module.

Table 10
Values of steam turbine model parameters for biomass power plants.

Constant	Value	Refs.	Year
T_g	0.2 s	[173]	2003
T_g	0.08 s	[171]	2018
T_{CH}	0.55 s	[173]	2003
T_{CH}	0.3 s	[171]	2018
T_{RH}	10 s	[171]	2018
F_{HP}	0.3	[171]	2018

Table 11
Values of non-reheat steam turbine parameters for CSPP.

Parameter	Value	Refs.	Year
T_g	1 s	[176]	2015
T_g	1 s	[181]	2018
T_{CH}	3 s	[176]	2015
T_{CH}	5 s	[79]	2017
T_{CH}	3 s	[181]	2018

4.4. Emerging renewable technologies

Biomass power plants are based on a conventional Rankine thermodynamic power cycle [105]. These power plants include a boiler, a steam turbine, and a condenser [167–170]. As a result, the models presented in Fig. 3 for steam turbines are used to simulate biomass power plants in frequency studies with the parameters shown in Table 10 [132,171,172].

Concentrated-solar power plants (CSPP) are based on heating a working fluid through concentrated sunlight. This heated fluid is then used with conventional turbines and generators to produce electricity [174]. Indeed, the solar heat from the field can be integrated into the three power conversion cycles of Section 3 [175]. However, they are commonly based on steam turbines [105]. Actually, in recent years, several studies focused on frequency control have included CSPP by using the non-reheat steam turbine shown in Fig. 3(a) [176–182]. The parameters used in this case are presented in Table 11. Rahman et al. [79] did not consider the governor transfer function.

Finally, and apart from the aforementioned vRES, biomass, and CSPP, there are other renewable sources, such as geothermal energy and ocean energy (tide and wave) [183]. However, and due to the low penetration of these sources and their weak integration, they are not considered in this study.

5. Simulation results

In order to understand the influence of the different values for the same parameter, some simulations are here carried out. Only those linear models which have severe differences between the values proposed in the specific literature are considered (i.e., Figs. 2, 3, 7 and 8). The values are changed between the minimum and the maximum of those

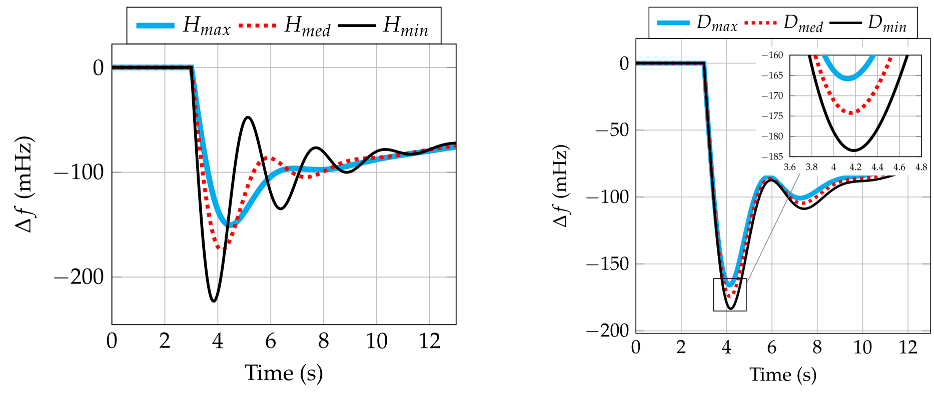

(a) H_{eq} (b) D

Fig. 12. Δf depending on the values of the power system.

Table 12
Values considered for comparing frequency stability.

Type	Figure	Parameter	Minimum	Maximum	Mean
Power system	2(a)	H_{eq}	3.00	7.11	5.06
		D	0.01	1.80	0.90
Non-reheat steam turbine	3(a)	T_g	0.06	0.40	0.23
		T_{CH}	0.17	0.60	0.39
Reheat steam turbine	3(b)	T_g	0.08	0.20	0.14
		T_{CH}	0.30	0.70	0.50
		T_{RH}	4.00	10.00	7.00
		F_{HP}	0.30	0.50	0.40
Hydro-power	7	T_g	0.20	0.60	0.40
		T_w	0.50	4.00	2.25
		T_R	–	–	5.00
		R_T	–	–	0.38
		R_P	–	–	0.05
Wind	8	K_{WTG}	–	–	1.00
		T_{WTG}	0.20	1.50	0.85

shown in previous tables, and the mean of them. Table 12 presents the specific values considered. In such cases where only one value is provided for a parameter, it is shown in the **Mean** column. To clearly show how the values affect the frequency stability, each parameter under analysis is changed at a time, considering the others as fixed and equal to the **Mean** values. A sudden increase of the consumed power is supposed at $t = 5$ s, with a value of $\Delta P = 0.05$ pu. This power imbalance is not considered for the wind turbine model, but a variable wind speed profile, as depicted in Fig. 16(a). Together with this, the primary and secondary frequency controls are included for thermal and hydropower plants, considering $R_{thermal} = R_{hydro} = 0.05$ for the primary frequency control, and an integral constant of $K_{I,thermal} = K_{I,hydro} = 1$. The results for the different simulations are shown in Figs. 12–16.

As can be seen, the reduction of the inertia H_{eq} causes an increase in the frequency deviation values and oscillations. This is in line with previous studies, as already explained in Section 1, and one of the main drawbacks of massive integration of vRES. Indeed, severe frequency variations can occur if proper controllers are not included in such units and vRES replace conventional power plants. With regard to the damping factor D, the lower its value the larger the frequency excursions, but its impact is much more reduced than H_{eq} (see Fig. 12. With regard to the non-reheat steam turbine model, both T_g and T_{CH} get lower and less oscillating frequency deviations when their values are reduced. In fact, both of them have nearly the same effects on frequency deviations, as their values are quite similar (refer to Table 12). Similar results are gotten for the reheat steam turbine (Fig. 14): T_g, T_{CH}, and T_{RH} reduce the Δf as they reduce their values, being T_{CH} the one that affects the most; however, the lower the value of F_{HP}, the larger the frequency excursion. The T_g value of hydropower plants slightly affects the frequency variation, whereas reducing the T_w constant reduces the Δf deviation as well (Fig. 15). Finally, as the value of T_{wtg} is reduced, the frequency excursions are increased (see Fig. 16). In summary, the analyzed parameters have a relevant influence on the frequency excursions and power system performance under imbalance conditions. Subsequently, standard benchmark models should be proposed by the researchers and the international committees for frequency control analysis, avoiding discrepancies in terms of simulation conditions, modeling and parameters.

6. Discussion

Apart from the different supply-side models presented in Sections 3 and 4, there are other elements, techniques, and power plants that can be considered in frequency deviation studies, which, in fact, can reduce the frequency excursions under high vRES integration [184]. With regard to energy storage systems (ESS), different solutions have been proposed in the literature to be applied to power systems with high RES integration, mainly batteries, super-capacitors, and flywheels. Nevertheless, these ESS require capital investment, being crucial to estimate the reasonable storage capacities avoiding any overflow size [185]. Among them, batteries are considered as the oldest and most mature storage system [186] and, according to Akram et al. [187], those based on lithium-ion are the ones that best suits for frequency regulation services. As super-capacitors have higher levels of power with lower energy storage ratio in contrast to batteries [188–190], several proposals have been made to combine batteries and super-capacitors [191], being considered as an interesting solution to solve the 'intermittency' of vRES [192]; in fact, according to Bai et al.[193], such combination is a proper alternative to improve the battery lifetime and enhance the system economy. Flywheels are applied from very small microsatellites to large power systems [194]. Amiryar and Pullen [195] concluded that flywheels are excellent options to back up solar PV.

Together with this, new types of hybrid power plants can deal with the power variations due to the high vRES integration. In fact, the pumped storage hydropower plants are commonly under study [196–199]. In fact, several advantages are obtained in contrast to other ESS, such as the huge amount of energy that can be stored in the reservoirs, the high energy conversion efficiency, and the flexibility provided in the short-term [200]. This kind of hybrid power plant helps on balancing the energy production and consumption by pumping water (increasing the load) at valley hours and generating electricity (increasing the generation) at peak hours, to balance energy production and consumption levels [201].

Hydrogen is the most abundant element on the Earth, accounting for, approximately, 15 mol% of its surface [202]. Nowadays, the

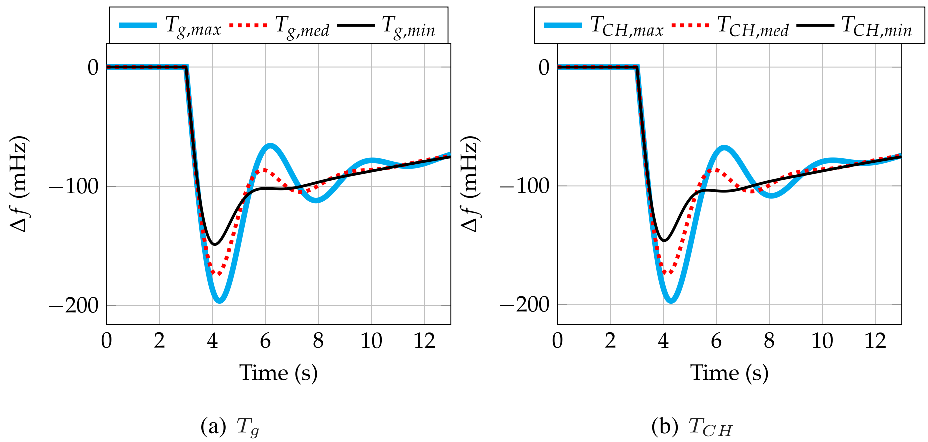

Fig. 13. Δf depending on the values of the non-reheat steam turbine.

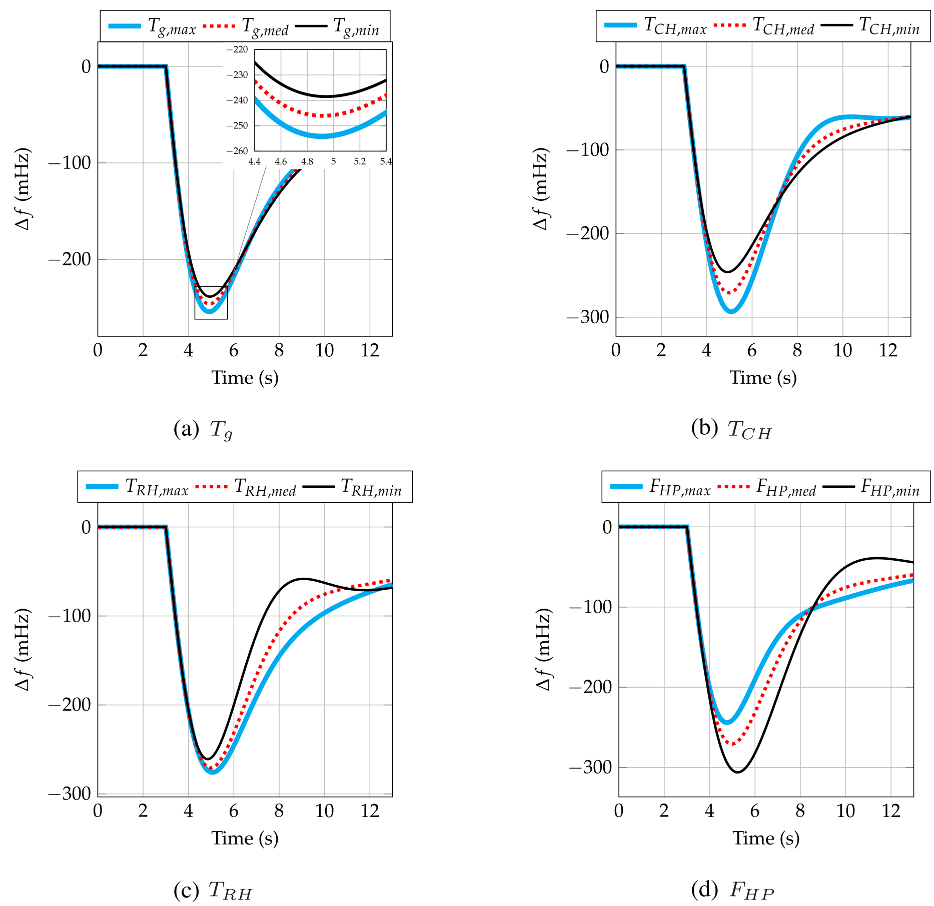

Fig. 14. Δf depending on the values of the reheat steam turbine.

'number-one element' is considered as the future energy carrier [203]. In fact, according to Mazloomi and Gomes [204], hydrogen can not only be a feasible energy carrier, but also an energy source at consumer level. Moreover, recent studies affirm that it can be produced from the different RES, such as solar and wind energies, water electrolysis, and biomass [205,206]. Among the different benefits of hydrogen, its main application from the power system stability point of view is the power-to-gas (P2G) conversion. P2G implies using the excess of generated renewable electricity to produce hydrogen via water electrolysis [207,208]. Hence, the system's flexibility would be enhanced [209], as these P2G plants would provide supply security in terms of storage facilities [210].

Finally, demand response participation in frequency control has gained important developments in recent years. A review of design and control schemes for electrical load contribution can be found in [211], focused on frequency control algorithms. Secondary frequency control based on demand response was developed by Lakshmanan et al. [212]. Control strategies for including battery energy storage systems (BESSs) and demand response for load frequency control strategies are recently proposed in [213–215]. Coordinated electric vehicles (dis)charging and demand response participating in frequency control have been also discussed in the specific literature [216–218]. In general, the contributions demonstrate the effectiveness of the coordinated and hybrid

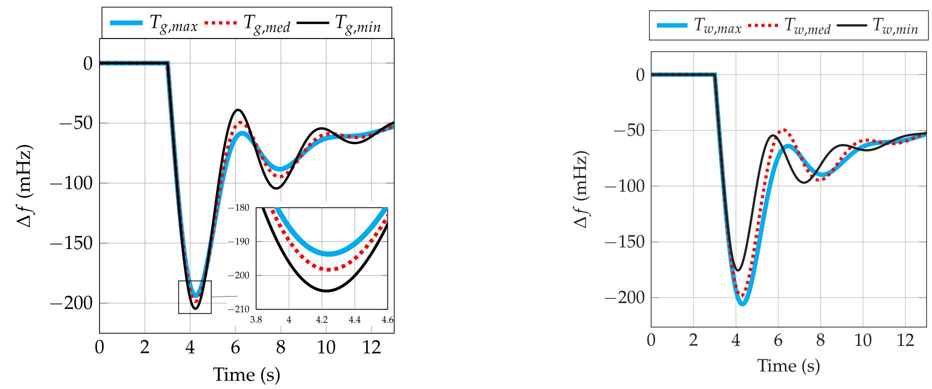

(a) T_g (b) T_w

Fig. 15. Δf depending on the values of the hydropower plant.

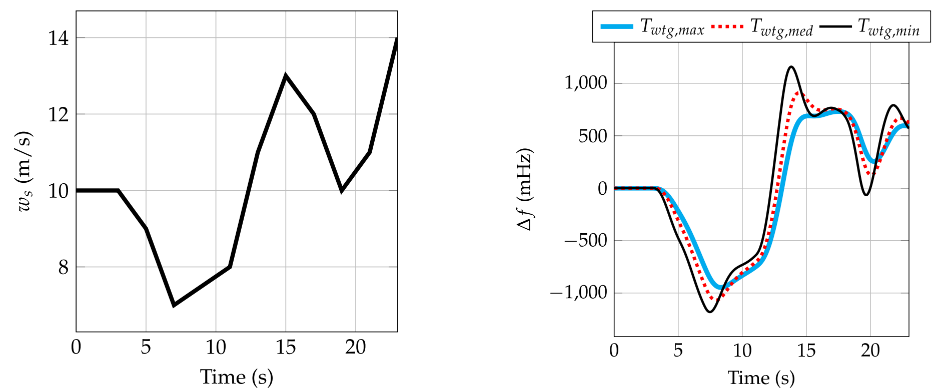

(a) s_w (b) T_{wtg}

Fig. 16. Δf depending on the values of the wind turbine generator.

algorithms, aimed to provide interactive solutions based on aggregated agents: demand response, energy storage and electric vehicles [219].

7. Conclusion

In this paper, an extensive literature review focused on supply-side and power system modeling for frequency control analysis is discussed in detail. The parameters involved in the swing equation (grid inertia and damping factor) are summarized and compared when used to simulate power systems. Moreover, the models for conventional generation units (steam turbines, gas turbines, combined cycle gas turbines, and nuclear power plants) and renewable generation units (mainly hydropower, wind and PV) are provided. The parameters used for each model are widely discussed and compared, with more than 50 different values identified and referenced. From this literature review, consensual models for the power system and the different generation units should be proposed, aiming to homogenize the frequency stability analysis that would allow the scientific community to evaluate future frequency control strategies under similar/equivalent assumptions, which is not currently available in the specific literature.

Declaration of competing interest

The authors declare that they have no known competing financial interests or personal relationships that could have appeared to influence the work reported in this paper.

References

[1] B.M. Weedy, B.J. Cory, N. Jenkins, J.B. Ekanayake, G. Strbac, Electric Power Systems, John Wiley & Sons, 2012.
[2] D. Greenwood, K. Lim, C. Patsios, P. Lyons, Y. Lim, P. Taylor, Frequency response services designed for energy storage, Appl. Energy 203 (2017) 115–127, http://dx.doi.org/10.1016/j.apenergy.2017.06.046.
[3] A. Ulbig, T.S. Borsche, G. Andersson, Impact of low rotational inertia on power system stability and operation, IFAC Proc. Vol. 47 (3) (2014) 7290–7297.
[4] A. Fathi, Q. Shafiee, H. Bevrani, Robust frequency control of microgrids using an extended virtual synchronous generator, IEEE Trans. Power Syst. 33 (6) (2018) 6289–6297.
[5] M. Dreidy, H. Mokhlis, S. Mekhilef, Inertia response and frequency control techniques for renewable energy sources: A review, Renew. Sustain. Energy Rev. 69 (2017) 144–155, http://dx.doi.org/10.1016/j.rser.2016.11.170.
[6] M. Alizadeh, M. Parsa Moghaddam, N. Amjady, P. Siano, M. Sheikh-El-Eslami, Flexibility in future power systems with high renewable penetration: A review, Renew. Sustain. Energy Rev. 57 (2016) 1186–1193, http://dx.doi.org/10.1016/j.rser.2015.12.200.
[7] S. Müller, The Power of Transformation: Wind, Sun, and the Economics of Flexible Power Systems, International Energy Agency, 2014.
[8] S. Impram, S. Varbak Nese, B. Oral, Challenges of renewable energy penetration on power system flexibility: A survey, Energy Strategy Rev. 31 (2020) 100539, http://dx.doi.org/10.1016/j.esr.2020.100539.
[9] H. Karbouj, Z.H. Rather, D. Flynn, H.W. Qazi, Non-synchronous fast frequency reserves in renewable energy integrated power systems: A critical review, Int. J. Electr. Power Energy Syst. 106 (2019) 488–501, http://dx.doi.org/10.1016/j.ijepes.2018.09.046.
[10] Y. Cheng, R. Azizipanah-Abarghooee, S. Azizi, L. Ding, V. Terzija, Smart frequency control in low inertia energy systems based on frequency response techniques: A review, Appl. Energy 279 (2020) 115798.
[11] Z. Wu, W. Gao, T. Gao, W. Yan, H. Zhang, S. Yan, X. Wang, State-of-the-art review on frequency response of wind power plants in power systems, J. Mod. Power Syst. Clean Energy 6 (1) (2018) 1–16, http://dx.doi.org/10.1007/s40565-017-0315-y.

[12] P. Sonkar, O. Rahi, Contribution of wind power plants in grid frequency regulation: Current perspective and future challenges, Wind Eng. 11 (2020) http://dx.doi.org/10.1177/0309524X19892899.

[13] F. Jibji-Bukar, O. Anaya-Lara, Frequency support from photovoltaic power plants using offline maximum power point tracking and variable droop control, IET Renew. Power Gener. 13 (2019) 2278–2286, http://dx.doi.org/10.1049/iet-rpg.2019.0211, (8).

[14] N. Mansouri, A. Lashab, J.M. Guerrero, A. Cherif, Photovoltaic power plants in electrical distribution networks: a review on their impact and solutions, IET Renew. Power Gener. 14 (2020) 2114–2125, http://dx.doi.org/10.1049/iet-rpg.2019.1172, (11).

[15] S.K. Jain, S. Chakrabarti, S. Singh, Review of load frequency control methods, Part-I: Introduction and pre-deregulation scenario, in: 2013 International Conference on Control, Automation, Robotics and Embedded Systems (CARE), IEEE, 2013, pp. 1–5.

[16] S.K. Pandey, S.R. Mohanty, N. Kishor, A literature survey on load–frequency control for conventional and distribution generation power systems, Renew. Sustain. Energy Rev. 25 (2013) 318–334.

[17] A. Pappachen, A.P. Fathima, Critical research areas on load frequency control issues in a deregulated power system: A state-of-the-art-of-review, Renew. Sustain. Energy Rev. 72 (2017) 163–177.

[18] H.H. Alhelou, M.-E. Hamedani-Golshan, R. Zamani, E. Heydarian-Forushani, P. Siano, Challenges and opportunities of load frequency control in conventional, modern and future smart power systems: A comprehensive review, Energies 11 (10) (2018) 2497.

[19] A. Fernández-Guillamón, E. Gómez-Lázaro, E. Muljadi, A. Molina-García, Power systems with high renewable energy sources: A review of inertia and frequency control strategies over time, Renew. Sustain. Energy Rev. 115 (2019) 109369.

[20] P. Li, W. Hu, R. Hu, Q. Huang, J. Yao, Z. Chen, Strategy for wind power plant contribution to frequency control under variable wind speed, Renew. Energy 130 (2019) 1226–1236.

[21] P. Kundur, N.J. Balu, M.G. Lauby, Power System Stability and Control, Vol. 7, McGraw-hill, New York, 1994.

[22] D. Obradović, M. Ghandhari, R. Eriksson, Assessment and design of frequency containment reserves with HVDC interconnections, in: 2018 North American Power Symposium (NAPS), IEEE, 2018, pp. 1–6.

[23] A. Fernández-Guillamón, J.I. Sarasúa, M. Chazarra, A. Vigueras-Rodríguez, D. Fernández-Muñoz, A. Molina-García, Frequency control analysis based on unit commitment schemes with high wind power integration: A Spanish isolated power system case study, Int. J. Electr. Power Energy Syst. 121 (2020) 106044.

[24] J.I. Sarasua, G. Martínez-Lucas, H. García-Pereira, G. Navarro-Soriano, A. Molina-García, A. Fernández-Guillamón, Hybrid frequency control strategies based on hydro-power, wind, and energy storage systems: Application to 100% renewable scenarios, IET Renew. Power Gener. (2021).

[25] N. Jaleeli, L.S. VanSlyck, D.N. Ewart, L.H. Fink, A.G. Hoffmann, Understanding automatic generation control, IEEE Trans. Power Syst. 7 (3) (1992) 1106–1122.

[26] A. Fernández Guillamón, New Contributions to Frequency Control Based on Virtual Synchronous Generators: Application to Power Systems with High Renewable Energy Sources Integration (Ph.D. thesis), Universidad Politécnica de Cartagena, 2020.

[27] N. Kakimoto, S. Takayama, H. Satoh, K. Nakamura, Power modulation of photovoltaic generator for frequency control of power system, IEEE Trans. Energy Convers. 24 (4) (2009) 943–949.

[28] M.I. Alomoush, Load frequency control and automatic generation control using fractional-order controllers, Electr. Eng. 91 (7) (2010) 357–368.

[29] M. Farahani, S. Ganjefar, M. Alizadeh, PID controller adjustment using chaotic optimisation algorithm for multi-area load frequency control, IET Control Theory Appl. 6 (13) (2012) 1984–1992.

[30] R. Farhangi, M. Boroushaki, S.H. Hosseini, Load–frequency control of interconnected power system using emotional learning-based intelligent controller, Int. J. Electr. Power Energy Syst. 36 (1) (2012) 76–83.

[31] Z. Akhtar, B. Chaudhuri, S.Y.R. Hui, Primary frequency control contribution from smart loads using reactive compensation, IEEE Trans. Smart Grid 6 (5) (2015) 2356–2365.

[32] N. Nguyen, J. Mitra, An analysis of the effects and dependency of wind power penetration on system frequency regulation, IEEE Trans. Sustain. Energy 7 (1) (2015) 354–363.

[33] M. Deepak, R.J. Abraham, F.M. Gonzalez-Longatt, D.M. Greenwood, H.-S. Rajamani, A novel approach to frequency support in a wind integrated power system, Renew. Energy 108 (2017) 194–206.

[34] M.H. Khooban, T. Niknam, F. Blaabjerg, T. Dragičević, A new load frequency control strategy for micro-grids with considering electrical vehicles, Electr. Power Syst. Res. 143 (2017) 585–598.

[35] K. Liao, Y. Xu, A robust load frequency control scheme for power systems based on second-order sliding mode and extended disturbance observer, IEEE Trans. Ind. Inf. 14 (7) (2017) 3076–3086.

[36] C. Peng, J. Zhang, H. Yan, Adaptive event-triggering H_∞ load frequency control for network-based power systems, IEEE Trans. Ind. Electron. 65 (2) (2017) 1685–1694.

[37] Y. Wang, H. Li, Y. Xu, Y. Tang, System frequency regulation in Singapore using distributed energy storage systems, in: 2017 Asian Conference on Energy, Power and Transportation Electrification (ACEPT), IEEE, 2017, pp. 1–6.

[38] A. Fernández-Guillamón, J. Villena-Lapaz, A. Vigueras-Rodríguez, T. García-Sánchez, A. Molina-García, An adaptive frequency strategy for variable speed wind turbines: application to high wind integration into power systems, Energies 11 (6) (2018) 1436.

[39] A. Fernández-Guillamón, A. Vigueras-Rodríguez, E. Gómez-Lázaro, A. Molina-García, Fast power reserve emulation strategy for VSWT supporting frequency control in multi-area power systems, Energies 11 (10) (2018) 2775.

[40] M.A. Mohamed, A.A.Z. Diab, H. Rezk, T. Jin, A novel adaptive model predictive controller for load frequency control of power systems integrated with DFIG wind turbines, Neural Comput. Appl. (2019) 1–11.

[41] I. Muñoz Benavente, A.D. Hansen, E. Gómez-Lázaro, T. García-Sánchez, A. Fernández-Guillamón, A. Molina-García, Impact of combined demand-response and wind power plant participation in frequency control for multi-area power systems, Energies 12 (9) (2019) 1687.

[42] C. Pradhan, C.N. Bhende, Online load frequency control in wind integrated power systems using modified Jaya optimization, Eng. Appl. Artif. Intell. 77 (2019) 212–228.

[43] M.H. Fini, M.E.H. Golshan, Determining optimal virtual inertia and frequency control parameters to preserve the frequency stability in islanded microgrids with high penetration of renewables, Electr. Power Syst. Res. 154 (2018) 13–22.

[44] B. Agrawal, Damping representation for power system stability studies, IEEE Power Eng. Rev. 18 (6) (1998) 41.

[45] C.-K. Zhang, L. Jiang, Q. Wu, Y. He, M. Wu, Further results on delay-dependent stability of multi-area load frequency control, IEEE Trans. Power Syst. 28 (4) (2013) 4465–4474.

[46] A.M. Howlader, Y. Izumi, A. Uehara, N. Urasaki, T. Senjyu, A.Y. Saber, A robust H∞ controller based frequency control approach using the wind-battery coordination strategy in a small power system, Int. J. Electr. Power Energy Syst. 58 (2014) 190–198.

[47] A. Molina-García, I. Munoz-Benavente, A.D. Hansen, E. Gómez-Lázaro, Demand-side contribution to primary frequency control with wind farm auxiliary control, IEEE Trans. Power Syst. 29 (5) (2014) 2391–2399.

[48] J. Pahasa, I. Ngamroo, Coordinated control of wind turbine blade pitch angle and PHEVs using MPCs for load frequency control of microgrid, IEEE Syst. J. 10 (1) (2014) 97–105.

[49] J. Zhong, L. He, C. Li, Y. Cao, J. Wang, B. Fang, L. Zeng, G. Xiao, Coordinated control for large-scale EV charging facilities and energy storage devices participating in frequency regulation, Appl. Energy 123 (2014) 253–262.

[50] M.F.M. Arani, Y.A.-R.I. Mohamed, Cooperative control of wind power generator and electric vehicles for microgrid primary frequency regulation, IEEE Trans. Smart Grid 9 (6) (2017) 5677–5686.

[51] P. Ojaghi, M. Rahmani, LMI-based robust predictive load frequency control for power systems with communication delays, IEEE Trans. Power Syst. 32 (5) (2017) 4091–4100.

[52] A.E. Onyeka, Y. Xing-Gang, Z. Mao, B. Jiang, Q. Zhang, Robust decentralised load frequency control for interconnected time delay power systems using sliding mode techniques, IET Control Theory Appl. (2019).

[53] J. Liu, Y. Gu, L. Zha, Y. Liu, J. Cao, Event-triggered H_∞ load frequency control for multiarea power systems under hybrid cyber attacks, IEEE Trans. Syst. Man Cybern.: Syst. 49 (8) (2019) 1665–1678.

[54] X. Shang-Guan, Y. He, C. Zhang, L. Jiang, J.W. Spencer, M. Wu, Sampled-data based discrete and fast load frequency control for power systems with wind power, Appl. Energy 259 (2020) 114202.

[55] K. Sudha, R.V. Santhi, Load frequency control of an interconnected reheat thermal system using type-2 fuzzy system including SMES units, Int. J. Electr. Power Energy Syst. 43 (1) (2012) 1383–1392.

[56] W. Tan, H. Zhang, M. Yu, Decentralized load frequency control in deregulated environments, Int. J. Electr. Power Energy Syst. 41 (1) (2012) 16–26.

[57] W. Tan, H. Zhou, Robust analysis of decentralized load frequency control for multi-area power systems, Int. J. Electr. Power Energy Syst. 43 (1) (2012) 996–1005.

[58] G.C. Sekhar, R.K. Sahu, A. Baliarsingh, S. Panda, Load frequency control of power system under deregulated environment using optimal firefly algorithm, Int. J. Electr. Power Energy Syst. 74 (2016) 195–211.

[59] R.K. Selvaraju, G. Somaskandan, Impact of energy storage units on load frequency control of deregulated power systems, Energy 97 (2016) 214–228.

[60] D. Saha, L.C. Saikia, Automatic generation control of a multi-area CCGT-thermal power system using stochastic search optimised integral minus proportional derivative controller under restructured environment, IET Gener. Transm. Distrib. 11 (15) (2017) 3801–3813.

[61] D. Saha, L.C. Saikia, Automatic generation control of an interconnected CCGT-thermal system using stochastic fractal search optimized classical controllers, Int. Trans. Electr. Energy Syst. 28 (5) (2018) e2533.

[62] H.M. Hasanien, A.A. El-Fergany, Salp swarm algorithm-based optimal load frequency control of hybrid renewable power systems with communication delay and excitation cross-coupling effect, Electr. Power Syst. Res. 176 (2019) 105938.

[63] K. Lu, W. Zhou, G. Zeng, Y. Zheng, Constrained population extremal optimization-based robust load frequency control of multi-area interconnected power system, Int. J. Electr. Power Energy Syst. 105 (2019) 249–271.
[64] S. Saxena, Load frequency control strategy via fractional-order controller and reduced-order modeling, Int. J. Electr. Power Energy Syst. 104 (2019) 603–614.
[65] J. Yang, Z. Zeng, Y. Tang, J. Yan, H. He, Y. Wu, Load frequency control in isolated micro-grids with electrical vehicles based on multivariable generalized predictive theory, Energies 8 (3) (2015) 2145–2164, http://dx.doi.org/10.3390/en8032145.
[66] W.E. Addisu, Intelligent Load Frequency Control in an Isolated Wind-Solar PV-Micro Turbine-Diesel Based Micro-Grid using V2G Integration (Master's thesis), UiT Norges arktiske universitet, 2017.
[67] G.S. Misyris, S. Chatzivasileiadis, T. Weckesser, Robust frequency control for varying inertia power systems, in: 2018 IEEE PES Innovative Smart Grid Technologies Conference Europe (ISGT-Europe), IEEE, 2018, pp. 1–6.
[68] H. Huang, F. Li, Sensitivity analysis of load-damping characteristic in power system frequency regulation, IEEE Trans. Power Syst. 28 (2) (2012) 1324–1335.
[69] Y. Wang, B. Liu, S. Duan, Modified virtual inertia control method of VSG strategy with improved transient response and power-supporting capability, IET Power Electron. 12 (12) (2019) 3178–3184.
[70] T. Kerdphol, F.S. Rahman, M. Watanabe, Y. Mitani, D. Turschner, H.-P. Beck, Enhanced virtual inertia control based on derivative technique to emulate simultaneous inertia and damping properties for microgrid frequency regulation, IEEE Access 7 (2019) 14422–14433.
[71] Y. Wang, X. Wang, Z. Chen, F. Blaabjerg, Small-signal stability analysis of inverter-fed power systems using component connection method, IEEE Trans. Smart Grid 9 (5) (2018) 5301–5310, http://dx.doi.org/10.1109/TSG.2017.2686841.
[72] V. Veerasamy, N.I.A. Wahab, R. Ramachandran, M.L. Othman, H. Hizam, A.X.R. Irudayaraj, J.M. Guerrero, J.S. Kumar, A Hankel matrix based reduced order model for stability analysis of hybrid power system using PSO-GSA optimized cascade PI-PD controller for automatic load frequency control, IEEE Access 8 (2020) 71422–71446, http://dx.doi.org/10.1109/ACCESS.2020.2987387.
[73] D. Ortiz-Villalba, C. Rahmann, R. Alvarez, C.A. Canizares, C. Strunck, Practical framework for frequency stability studies in power systems with renewable energy sources, IEEE Access 8 (2020) 202286–202297, http://dx.doi.org/10.1109/ACCESS.2020.3036162.
[74] J. Chen, M. Liu, F. Milano, Aggregated model of virtual power plants for transient frequency and voltage stability analysis, IEEE Trans. Power Syst. 36 (5) (2021) 4366–4375, http://dx.doi.org/10.1109/TPWRS.2021.3063280.
[75] H. Zhang, J. Liu, S. Xu, Practical stability and event-triggered load frequency control of networked power systems, IEEE Trans. Syst. Man Cybern.: Syst. (2022) 1–9, http://dx.doi.org/10.1109/TSMC.2022.3143853.
[76] A. Khodabakhshian, N. Golbon, Unified PID design for load frequency control, in: Proceedings of the 2004 IEEE International Conference on Control Applications, 2004. Vol. 2, IEEE, 2004, pp. 1627–1632.
[77] A. Zertec, G. Verbic, M. Pantos, Optimised control approach for frequency–control of variable speed wind turbines, IET Renew. Power Gener. 6 (1) (2012) 17–23.
[78] L.C. Saikia, S.K. Sahu, Automatic generation control of a combined cycle gas turbine plant with classical controllers using firefly algorithm, Int. J. Electr. Power Energy Syst. 53 (2013) 27–33.
[79] A. Rahman, L.C. Saikia, N. Sinha, Automatic generation control of an interconnected two-area hybrid thermal system considering dish-stirling solar thermal and wind turbine system, Renew. Energy 105 (2017) 41–54.
[80] X. Wang, Y. Wang, Y. Liu, Dynamic load frequency control for high-penetration wind power considering wind turbine fatigue load, Int. J. Electr. Power Energy Syst. 117 (2020) 105696.
[81] M.R. Hazari, E. Jahan, M.A. Mannan, J. Tamura, Coordinated control scheme of battery storage system to augment LVRT capability of SCIG-based wind turbines and frequency regulation of hybrid power system, Electronics 9 (2) (2020) http://dx.doi.org/10.3390/electronics9020239.
[82] F. Díaz-González, M. Hau, A. Sumper, O. Gomis-Bellmunt, Participation of wind power plants in system frequency control: Review of grid code requirements and control methods, Renew. Sustain. Energy Rev. 34 (2014) 551–564, http://dx.doi.org/10.1016/j.rser.2014.03.040.
[83] L. Wang, Z. Yang, S. Sharma, A. Mian, T.-E. Lin, G. Tsatsaronis, F. Maréchal, Y. Yang, A review of evaluation, optimization and synthesis of energy systems: Methodology and application to thermal power plants, Energies 12 (1) (2019) http://dx.doi.org/10.3390/en12010073.
[84] https://www.worldcoal.org/coal/uses-coal/coal-electricity.
[85] M. Eremia, M. Shahidehpour, Handbook of Electrical Power System Dynamics: Modeling, Stability, and Control, Vol. 92, John Wiley & Sons, 2013.
[86] H.A. Yousef, A.-K. Khalfan, M.H. Albadi, N. Hosseinzadeh, Load frequency control of a multi-area power system: An adaptive fuzzy logic approach, IEEE Trans. Power Syst. 29 (4) (2014) 1822–1830.
[87] H. Yousef, Adaptive fuzzy logic load frequency control of multi-area power system, Int. J. Electr. Power Energy Syst. 68 (2015) 384–395.
[88] K.K. Challa, P.N. Rao, Analysis and design of controller for two area thermal-hydro-gas AGC system, in: 2010 Joint International Conference on Power Electronics, Drives and Energy Systems & 2010 Power India, IEEE, 2010, pp. 1–4.
[89] K.S. Parmar, S. Majhi, D. Kothari, Load frequency control of a realistic power system with multi-source power generation, Int. J. Electr. Power Energy Syst. 42 (1) (2012) 426–433.
[90] B. Mohanty, S. Panda, P. Hota, Controller parameters tuning of differential evolution algorithm and its application to load frequency control of multi-source power system, Int. J. Electr. Power Energy Syst. 54 (2014) 77–85.
[91] G. Lalor, M. O'Malley, Frequency control on an island power system with increasing proportions of combined cycle gas turbines, in: 2003 IEEE Bologna Power Tech Conference Proceedings, Vol. 4, IEEE, 2003, pp. 7–pp.
[92] G. Lalor, J. Ritchie, D. Flynn, M.J. O'Malley, The impact of combined-cycle gas turbine short-term dynamics on frequency control, IEEE Trans. Power Syst. 20 (3) (2005) 1456–1464.
[93] L. Meegahapola, D. Flynn, Characterization of gas turbine lean blowout during frequency excursions in power networks, IEEE Trans. Power Syst. 30 (4) (2014) 1877–1887.
[94] M. Hermans, K. Bruninx, E. Delarue, Impact of CCGT start-up flexibility and cycling costs toward renewables integration, IEEE Trans. Sustain. Energy 9 (3) (2018) 1468–1476.
[95] A. Lokhov, Load-following with nuclear power plants, NEA News 29 (2) (2011) 18–20.
[96] Y. Dai, P. Jiang, L. Gao, W. Kan, X. Xiao, G. Jin, Capacity limitation of nuclear units in grid based on analysis of frequency regulation, Front. Energy 6 (2) (2012) 148–154.
[97] G. Lazarev, V. Hrustalyov, M. Garievskij, 1. Non-Baseload operation in nuclear power plants: Load following and frequency control modes of flexible operation, Nucl. Energy Ser. (2018) 173.
[98] T. Inoue, H. Amano, A thermal power plant model for dynamic simulation of load frequency control, in: 2006 IEEE PES Power Systems Conference and Exposition, IEEE, 2006, pp. 1442–1447.
[99] K. Shimizu, T. Masuta, Y. Ota, A. Yokoyama, A new load frequency control method in power system using vehicle-to-grid system considering users' convenience, in: Proceedings of the 17th Power System Computation Conference, Stockholm, Sweden, 2011, pp. 22–26.
[100] T. Masuta, A. Yokoyama, Supplementary load frequency control by use of a number of both electric vehicles and heat pump water heaters, IEEE Trans. Smart Grid 3 (3) (2012) 1253–1262.
[101] S. Takayama, R. Matsuhashi, Development of model for load frequency control in power system with large-scale integration of renewable energy, in: 2016 IEEE Power and Energy Conference at Illinois (PECI), IEEE, 2016, pp. 1–8.
[102] https://www.world-nuclear.org/.
[103] P. Wang, Y. Fu, X. Wei, F. Zhao, Simulation study of frequency control characteristics of a generation III+ nuclear power plant, Ann. Nucl. Energy 115 (2018) 502–522.
[104] G. Li, X. Wang, B. Liang, X. Li, B. Zhang, Y. Zou, Modeling and control of nuclear reactor cores for electricity generation: A review of advanced technologies, Renew. Sustain. Energy Rev. 60 (2016) 116–128, http://dx.doi.org/10.1016/j.rser.2016.01.116.
[105] M.J. Moran, M.B. Bailey, D.D. Boettner, H.N. Shapiro, Fundamentals of Engineering Thermodynamics, Wiley, 2018.
[106] D. Chaturvedi, R. Umrao, O. Malik, Adaptive polar fuzzy logic based load frequency controller, Int. J. Electr. Power Energy Syst. 66 (2015) 154–159.
[107] B. Mohanty, TLBO optimized sliding mode controller for multi-area multi-source nonlinear interconnected AGC system, Int. J. Electr. Power Energy Syst. 73 (2015) 872–881.
[108] V. Kumarakrishnan, G. Vijayakumar, D. Boopathi, K. Jagatheesan, S. Saravanan, B. Anand, Optimized PSO technique based PID controller for load frequency control of single area power system, Solid State Technol. 63 (5) (2020) 7979–7990.
[109] P.D. Lund, J. Lindgren, J. Mikkola, J. Salpakari, Review of energy system flexibility measures to enable high levels of variable renewable electricity, Renew. Sustain. Energy Rev. 45 (2015) 785–807, http://dx.doi.org/10.1016/j.rser.2015.01.057.
[110] M.S. Javed, T. Ma, J. Jurasz, M.Y. Amin, Solar and wind power generation systems with pumped hydro storage: Review and future perspectives, Renew. Energy 148 (2020) 176–192, http://dx.doi.org/10.1016/j.renene.2019.11.157.
[111] S. Garrido, T. Sequeira, M. Santos, Renewable energy and sustainability from the supply side: A critical review and analysis, Appl. Sci. 10 (17) (2020) http://dx.doi.org/10.3390/app10175755.
[112] A. Safaei, H.M. Roodsari, H.A. Abyaneh, Optimal load frequency control of an island small hydropower plant, in: The 3rd Conference on Thermal Power Plants, IEEE, 2011, pp. 1–6.
[113] Y. Xu, C. Li, Z. Wang, N. Zhang, B. Peng, Load frequency control of a novel renewable energy integrated micro-grid containing pumped hydropower energy storage, IEEE Access 6 (2018) 29067–29077.

[114] A. Femández-Guillamón, A. Molina-García, A. Vigueras-Rodríguez, E. GÓmez-Lázaro, Frequency response and inertia analysis in power systems with high wind energy integration, in: 2019 International Conference on Clean Electrical Power (ICCEP), IEEE, 2019, pp. 388–393.
[115] A. Fernández-Guillamón, G. Martínez-Lucas, A. Molina-García, J.-I. Sarasua, Hybrid wind–PV frequency control strategy under variable weather conditions in isolated power systems, Sustainability 12 (18) (2020) 7750.
[116] A. Fernández-Guillamón, A. Vigueras-Rodríguez, A. Molina-García, Análisis y Simulación de Estrategias Agregadas de Control de Frecuencia Entre Grandes Parques Eólicos y Aprovechamientos Hidroeléctricos (M.S. thesis), Universidad Politécnica de Cartagena, 2017.
[117] G. Martínez-Lucas, J.I. Sarasúa, J.A. Sánchez-Fernández, J.R. Wilhelmi, Power-frequency control of hydropower plants with long penstocks in isolated systems with wind generation, Renew. Energy 83 (2015) 245–255.
[118] G. Martínez-Lucas, J.I. Sarasúa, J.A. Sánchez-Fernández, Frequency regulation of a hybrid wind–hydro power plant in an isolated power system, Energies 11 (1) (2018) 239.
[119] J.I. Sarasúa, G. Martínez-Lucas, M. Lafoz, Analysis of alternative frequency control schemes for increasing renewable energy penetration in El Hierro Island power system, Int. J. Electr. Power Energy Syst. 113 (2019) 807–823.
[120] G. Shu-Feng, Z. Jie-Tan, A. Philip, H. Li-Li, J. Jing, A review of wind turbine deloaded operation techniques for primary frequency control in power system, in: 2018 China International Conference on Electricity Distribution (CICED), 2018, pp. 63–71, http://dx.doi.org/10.1109/CICED.2018.8592549.
[121] X.-y. Zhang, X.-b. Zhang, W.-q. Wang, S. Jiale, The study of on grid wind turbine generator made in China, in: 2010 Asia-Pacific Power and Energy Engineering Conference, IEEE, 2010, pp. 1–4.
[122] S. Li, T.A. Haskew, Energy capture, conversion, and control study of DFIG wind turbine under weibull wind distribution, in: 2009 IEEE Power & Energy Society General Meeting, IEEE, 2009, pp. 1–9.
[123] L. Li, B. Han, Y. Ren, J. Brindley, L. Jiang, An improved hybrid hill climb searching control for MPPT of wind power generation systems under fast varying wind speed, in: International Conference on Renewable Power Generation (RPG 2015), 2015, pp. 1–6, http://dx.doi.org/10.1049/cp.2015.0493.
[124] A. Zertek, G. Verbic, M. Pantos, A novel strategy for variable-speed wind turbines' participation in primary frequency control, IEEE Trans. Sustain. Energy 3 (4) (2012) 791–799.
[125] K. Vidyanandan, N. Senroy, Primary frequency regulation by deloaded wind turbines using variable droop, IEEE Trans. Power Syst. 28 (2) (2012) 837–846.
[126] M. Kayikçi, J.V. Milanovic, Dynamic contribution of DFIG-based wind plants to system frequency disturbances, IEEE Trans. Power Syst. 24 (2) (2009) 859–867.
[127] A. Attya, J. Domínguez-García, O. Anaya-Lara, A review on frequency support provision by wind power plants: Current and future challenges, Renew. Sustain. Energy Rev. 81 (2018) 2071–2087, http://dx.doi.org/10.1016/j.rser.2017.06.016.
[128] Z. Wu, W. Gao, T. Gao, State-of-the-art review on frequency response of wind power plants in power systems, J. Mod. Power Syst. Clean Energy 6 (2018) 1–16, http://dx.doi.org/10.1007/s40565-017-0315-y.
[129] L.-R. Chang-Chien, C.-C. Sun, Y.-J. Yeh, Modeling of wind farm participation in AGC, IEEE Trans. Power Syst. 29 (3) (2014) 1204–1211, http://dx.doi.org/10.1109/TPWRS.2013.2291397.
[130] L. Fernandez, C. Garcia, J. Saenz, F. Jurado, Equivalent models of wind farms by using aggregated wind turbines and equivalent winds, Energy Convers. Manage. 50 (3) (2009) 691–704.
[131] J. Conroy, R. Watson, Aggregate modelling of wind farms containing full-converter wind turbine generators with permanent magnet synchronous machines: transient stability studies, IET Renew. Power Gener. 3 (1) (2009) 39–52.
[132] M.M. Rahman, S. Mohammad, M.S. Hossain, Frequency control in micro grid system using solar, wind, fuel cell and biomass energy, in: 2018 International Conference on Innovation in Engineering and Technology (ICIET), IEEE, 2018, pp. 1–6.
[133] R. Ahmadi, A. Sheikholeslami, A. Nabavi Niaki, A. Ranjbar, Dynamic participation of doubly fed induction generators in multi-control area load frequency control, Int. Trans. Electr. Energy Syst. 25 (7) (2015) 1130–1147.
[134] L. Miao, J. Wen, H. Xie, C. Yue, W.-J. Lee, Coordinated control strategy of wind turbine generator and energy storage equipment for frequency support, IEEE Trans. Ind. Appl. 51 (4) (2015) 2732–2742.
[135] F. Hafiz, A. Abdennour, An adaptive neuro-fuzzy inertia controller for variable-speed wind turbines, Renew. Energy 92 (2016) 136–146.
[136] M. Persson, P. Chen, Frequency control by variable speed wind turbines in islanded power systems with various generation mix, IET Renew. Power Gener. 11 (8) (2016) 1101–1109.
[137] Y. Tang, Y. Bai, C. Huang, B. Du, Linear active disturbance rejection-based load frequency control concerning high penetration of wind energy, Energy Convers. Manage. 95 (2015) 259–271, http://dx.doi.org/10.1016/j.enconman.2015.02.005.
[138] A. Fernández-Guillamón, A. Vigueras-Rodríguez, A. Molina-García, Analysis of power system inertia estimation in high wind power plant integration scenarios, IET Renew. Power Gener. 13 (15) (2019) 2807–2816.
[139] A.D. Hansen, M. Altin, I.D. Margaris, F. Iov, G.C. Tarnowski, Analysis of the short-term overproduction capability of variable speed wind turbines, Renew. Energy 68 (2014) 326–336.
[140] J.W. Choi, S.Y. Heo, M.K. Kim, Hybrid operation strategy of wind energy storage system for power grid frequency regulation, IET Gener. Transm. Distrib. 10 (3) (2016) 736–749, http://dx.doi.org/10.1049/iet-gtd.2015.0149.
[141] D. Ochoa, S. Martinez, Fast-frequency response provided by DFIG-wind turbines and its impact on the grid, IEEE Trans. Power Syst. 32 (5) (2016) 4002–4011.
[142] A. Jafari, G. Shahgholian, Analysis and simulation of a sliding mode controller for mechanical part of a doubly-fed induction generator-based wind turbine, IET Gener. Transm. Distrib. 11 (10) (2017) 2677–2688.
[143] J. Liu, Y. Gao, S. Geng, L. Wu, Nonlinear control of variable speed wind turbines via fuzzy techniques, IEEE Access 5 (2017) 27–34.
[144] J. Fortmann, Modeling of Wind Turbines with Doubly Fed Generator System, Springer, 2014.
[145] F. Huerta, R.L. Tello, M. Prodanovic, Real-time power-hardware-in-the-loop implementation of variable-speed wind turbines, IEEE Trans. Ind. Electron. 64 (3) (2017) 1893–1904.
[146] W. Liu, Y. Liu, Hierarchical model predictive control of wind farm with energy storage system for frequency regulation during black-start, Int. J. Electr. Power Energy Syst. 119 (2020) 105893, http://dx.doi.org/10.1016/j.ijepes.2020.105893.
[147] S. Chalise, H.R. Atia, B. Poudel, R. Tonkoski, Impact of active power curtailment of wind turbines connected to residential feeders for overvoltage prevention, IEEE Trans. Sustain. Energy 7 (2) (2015) 471–479.
[148] M. Kheshti, L. Ding, W. Bao, M. Yin, Q. Wu, V. Terzija, Toward intelligent inertial frequency participation of wind farms for the grid frequency control, IEEE Trans. Ind. Inf. (2019) 1, http://dx.doi.org/10.1109/TII.2019.2924662.
[149] P. Li, W. Hu, R. Hu, Q. Huang, J. Yao, Z. Chen, Strategy for wind power plant contribution to frequency control under variable wind speed, Renew. Energy 130 (2019) 1226–1236, http://dx.doi.org/10.1016/j.renene.2017.12.046.
[150] N.R. Ullah, T. Thiringer, D. Karlsson, Temporary primary frequency control support by variable speed wind turbines—Potential and applications, IEEE Trans. Power Syst. 23 (2) (2008) 601–612.
[151] G.C. Tarnowski, P.C. Kjar, P.E. Sorensen, J. Ostergaard, Variable speed wind turbines capability for temporary over-production, in: 2009 IEEE Power & Energy Society General Meeting, IEEE, 2009, pp. 1–7.
[152] N.W. Miller, J.J. Sanchez-Gasca, W.W. Price, R.W. Delmerico, Dynamic modeling of GE 1.5 and 3.6 MW wind turbine-generators for stability simulations, in: 2003 IEEE Power Engineering Society General Meeting (IEEE Cat. No. 03CH37491), Vol. 3, IEEE, 2003, pp. 1977–1983.
[153] K. Clark, N.W. Miller, J.J. Sanchez-Gasca, Modeling of GE wind turbine-generators for grid studies, GE Energy 4 (2010) 0885–8950.
[154] P. Zarina, S. Mishra, P. Sekhar, Deriving inertial response from a non-inertial PV system for frequency regulation, in: 2012 IEEE International Conference on Power Electronics, Drives and Energy Systems (PEDES), IEEE, 2012, pp. 1–5.
[155] P. Zarina, S. Mishra, P. Sekhar, Photovoltaic system based transient mitigation and frequency regulation, in: 2012 Annual IEEE India Conference (INDICON), IEEE, 2012, pp. 1245–1249.
[156] H. Xin, Y. Liu, Z. Wang, D. Gan, T. Yang, A new frequency regulation strategy for photovoltaic systems without energy storage, IEEE Trans. Sustain. Energy 4 (4) (2013) 985–993.
[157] P. Zarina, S. Mishra, P. Sekhar, Exploring frequency control capability of a PV system in a hybrid PV-rotating machine-without storage system, Int. J. Electr. Power Energy Syst. 60 (2014) 258–267.
[158] C. Rahmann, A. Castillo, Fast frequency response capability of photovoltaic power plants: The necessity of new grid requirements and definitions, Energies 7 (10) (2014) 6306–6322.
[159] P. Moutis, A. Vassilakis, A. Sampani, N. Hatziargyriou, DC switch driven active power output control of photovoltaic inverters for the provision of frequency regulation, IEEE Trans. Sustain. Energy 6 (4) (2015) 1485–1493.
[160] M. Taghizadeh, M. Hoseintabar, J. Faiz, Frequency control of isolated WT/PV/SOFC/UC network with new control strategy for improving SOFC dynamic response, Int. Trans. Electr. Energy Syst. 25 (9) (2015) 1748–1770.
[161] A. Bakeer, G. Magdy, A. Chub, H. Bevrani, A sophisticated modeling approach for photovoltaic systems in load frequency control, Int. J. Electr. Power Energy Syst. 134 (2022) 107330, http://dx.doi.org/10.1016/j.ijepes.2021.107330.
[162] G. Magdy, A. Bakeer, M. Nour, E. Petlenkov, A new virtual synchronous generator design based on the SMES system for frequency stability of low-inertia power grids, Energies 13 (21) (2020) 5641.
[163] G. Magdy, G. Shabib, A.A. Elbaset, Y. Mitani, A novel coordination scheme of virtual inertia control and digital protection for microgrid dynamic security considering high renewable energy penetration, IET Renew. Power Gener. 13 (3) (2019) 462–474.
[164] M.H. Khooban, M. Gheisarnejad, A novel deep reinforcement learning controller based type-II fuzzy system: Frequency regulation in microgrids, IEEE Trans. Emerg. Top. Comput. Intell. (2020).
[165] H. Ali, G. Magdy, B. Li, G. Shabib, A.A. Elbaset, D. Xu, Y. Mitani, A new frequency control strategy in an islanded microgrid using virtual inertia control-based coefficient diagram method, IEEE Access 7 (2019) 16979–16990.

[166] T. Kerdphol, F.S. Rahman, Y. Mitani, M. Watanabe, S.K. Küfeoğlu, Robust virtual inertia control of an islanded microgrid considering high penetration of renewable energy, IEEE Access 6 (2017) 625–636.
[167] J.-H. Moon, J.-W. Lee, U.-D. Lee, Economic analysis of biomass power generation schemes under renewable energy initiative with Renewable Portfolio Standards (RPS) in Korea, Bioresour. Technol. 102 (20) (2011) 9550–9557.
[168] H.T. Luk, T.Y.G. Lam, A.O. Oyedun, T. Gebreegziabher, C.W. Hui, Drying of biomass for power generation: A case study on power generation from empty fruit bunch, Energy 63 (2013) 205–215.
[169] T. Gebreegziabher, A.O. Oyedun, H.T. Luk, T.Y.G. Lam, Y. Zhang, C.W. Hui, Design and optimization of biomass power plant, Chem. Eng. Res. Des. 92 (8) (2014) 1412–1427.
[170] N. Shabani, T. Sowlati, M. Ouhimmou, M. Rönnqvist, Tactical supply chain planning for a forest biomass power plant under supply uncertainty, Energy 78 (2014) 346–355.
[171] A.K. Barik, D.C. Das, Active power management of isolated renewable microgrid generating power from rooftop solar arrays, sewage waters and solid urban wastes of a smart city using salp swarm algorithm, in: 2018 Technologies for Smart-City Energy Security and Power (ICSESP), IEEE, 2018, pp. 1–6.
[172] T. Mahto, H. Malik, V. Mukherjee, Fractional order control and simulation of wind-biomass isolated hybrid power system using particle swarm optimization, in: Applications of Artificial Intelligence Techniques in Engineering, Springer, 2019, pp. 277–287.
[173] F. Jurado, J.R. Saenz, An adaptive control scheme for biomass-based diesel–wind system, Renew. Energy 28 (1) (2003) 45–57.
[174] K.M. Powell, K. Rashid, K. Ellingwood, J. Tuttle, B.D. Iverson, Hybrid concentrated solar thermal power systems: A review, Renew. Sustain. Energy Rev. 80 (2017) 215–237.
[175] O. Behar, Solar thermal power plants–A review of configurations and performance comparison, Renew. Sustain. Energy Rev. 92 (2018) 608–627.
[176] Y. Sharma, L.C. Saikia, Automatic generation control of a multi-area ST–Thermal power system using Grey Wolf Optimizer algorithm based classical controllers, Int. J. Electr. Power Energy Syst. 73 (2015) 853–862.
[177] R. Rajbongshi, L.C. Saikia, Combined control of voltage and frequency of multi-area multisource system incorporating solar thermal power plant using LSA optimised classical controllers, IET Gener. Transm. Distrib. 11 (10) (2017) 2489–2498.
[178] A. Saha, L.C. Saikia, Utilisation of ultra-capacitor in load frequency control under restructured STPP-thermal power systems using WOA optimised PIDN-FOPD controller, IET Gener. Transm. Distrib. 11 (13) (2017) 3318–3331.
[179] M.K. Debnath, S. Sinha, R.K. Mallick, Automatic generation control including solar thermal power generation with fuzzy–PID controller with derivative filter, Int. J. Renew. Energy Res. (IJRER) 8 (1) (2018) 26–35.
[180] X. Liao, K. Liu, L. Qin, N. Wang, Y. Ma, Z. Chen, K. Ding, Q. Zhou, Cooperative DMPC-based load frequency control of AC/DC interconnected power system with solar thermal power plant, in: 2018 IEEE PES Asia-Pacific Power and Energy Engineering Conference (APPEEC), IEEE, 2018, pp. 341–346.
[181] S. Ranjan, D.C. Das, S. Behera, N. Sinha, Parabolic trough solar–thermal–wind–diesel isolated hybrid power system: active power/frequency control analysis, IET Renew. Power Gener. 12 (16) (2018) 1893–1903.
[182] D. Mishra, T. Panigrahi, A. Mohanty, P. Ray, Teaching learning based optimization for frequency regulation in two area thermal-solar hybrid power system, in: Applications of Artificial Intelligence Techniques in Engineering, Springer, 2019, pp. 63–71.
[183] P.A. Owusu, S. Asumadu-Sarkodie, A review of renewable energy sources, sustainability issues and climate change mitigation, Cogent Eng. 3 (1) (2016) 1167990.
[184] Z.A. Obaid, L.M. Cipcigan, L. Abrahim, M.T. Muhssin, Frequency control of future power systems: reviewing and evaluating challenges and new control methods, J. Mod. Power Syst. Clean Energy 7 (1) (2019) 9–25.
[185] A. Tani, M.B. Camara, B. Dakyo, Energy management in the decentralized generation systems based on renewable energy—Ultracapacitors and battery to compensate the wind/load power fluctuations, IEEE Trans. Ind. Appl. 51 (2) (2015) 1817–1827.
[186] H. Chen, T.N. Cong, W. Yang, C. Tan, Y. Li, Y. Ding, Progress in electrical energy storage system: A critical review, Prog. Nat. Sci. 19 (3) (2009) 291–312, http://dx.doi.org/10.1016/j.pnsc.2008.07.014.
[187] U. Akram, M. Nadarajah, R. Shah, F. Milano, A review on rapid responsive energy storage technologies for frequency regulation in modern power systems, Renew. Sustain. Energy Rev. 120 (2020) 109626, http://dx.doi.org/10.1016/j.rser.2019.109626.
[188] J. Marcos, O. Storkël, L. Marroyo, M. Garcia, E. Lorenzo, Storage requirements for PV power ramp-rate control, Sol. Energy 99 (2014) 28–35.
[189] N.B. Salim, H. Aboelsoud, T. Tsuji, T. Oyama, K. Uchida, Load frequency control of two-area network using renewable energy resources and battery energy storage system, J. Electr. Syst. 13 (2) (2017).
[190] Z. Zhao, H. Xiao, Y. Yang, Improved coordinated control strategy of hybrid energy storages in PV Power Smoothing, Energy Procedia 145 (2018) 151–156.
[191] Z. Cabrane, M. Ouassaid, M. Maaroufi, Analysis and evaluation of battery-supercapacitor hybrid energy storage system for photovoltaic installation, Int. J. Hydrogen Energy 41 (45) (2016) 20897–20907, http://dx.doi.org/10.1016/j.ijhydene.2016.06.141.
[192] A. Chandra, Supercapacitors: An alternate technology for energy storage, Proc. Natl. Acad. Sci. 82 (2012) 79–90, http://dx.doi.org/10.1007/s40010-012-0009-9.
[193] L. Bai, F. Li, Q. Hu, H. Cui, X. Fang, Application of battery-supercapacitor energy storage system for smoothing wind power output: An optimal coordinated control strategy, in: 2016 IEEE Power and Energy Society General Meeting (PESGM), 2016, pp. 1–5.
[194] S.M. G, F. Faraji, A. Majazi, K. Al-Haddad, A comprehensive review of flywheel energy storage system technology, Renew. Sustain. Energy Rev. 67 (2017) 477–490, http://dx.doi.org/10.1016/j.rser.2016.09.060.
[195] M.E. Amiryar, K.R. Pullen, A review of flywheel energy storage system technologies and their applications, Appl. Sci. 7 (3) (2017) http://dx.doi.org/10.3390/app7030286.
[196] A.J. Duque, E.D. Castronuovo, I. Sánchez, J. Usaola, Optimal operation of a pumped-storage hydro plant that compensates the imbalances of a wind power producer, Electr. Power Syst. Res. 81 (9) (2011) 1767–1777.
[197] E. Muljadi, M. Singh, V. Gevorgian, M. Mohanpurkar, R. Hovsapian, V. Koritarov, Dynamic modeling of adjustable-speed pumped storage hydropower plant, in: 2015 IEEE Power & Energy Society General Meeting, IEEE, 2015, pp. 1–5.
[198] F. Petrakopoulou, A. Robinson, M. Loizidou, Simulation and analysis of a stand-alone solar-wind and pumped-storage hydropower plant, Energy 96 (2016) 676–683.
[199] G.E. Alvarez, Operation of pumped storage hydropower plants through optimization for power systems, Energy 202 (2020) 117797.
[200] J.I. Pérez-Díaz, M. Chazarra, J. García-González, G. Cavazzini, A. Stoppato, Trends and challenges in the operation of pumped-storage hydropower plants, Renew. Sustain. Energy Rev. 44 (2015) 767–784.
[201] H. Zhang, D. Chen, B. Xu, E. Patelli, S. Tolo, Dynamic analysis of a pumped-storage hydropower plant with random power load, Mech. Syst. Signal Process. 100 (2018) 524–533.
[202] K.T. Møller, T.R. Jensen, E. Akiba, H.-w. Li, Hydrogen-A sustainable energy carrier, Prog. Nat. Sci.: Mater. Int. 27 (1) (2017) 34–40.
[203] M.H. McCay, S. Shafiee, Hydrogen: An energy carrier, in: Future Energy, Elsevier, 2020, pp. 475–493.
[204] K. Mazloomi, C. Gomes, Hydrogen as an energy carrier: Prospects and challenges, Renew. Sustain. Energy Rev. 16 (5) (2012) 3024–3033.
[205] S.E. Hosseini, M.A. Wahid, Hydrogen production from renewable and sustainable energy resources: Promising green energy carrier for clean development, Renew. Sustain. Energy Rev. 57 (2016) 850–866.
[206] S.E. Hosseini, M.A. Wahid, Hydrogen from solar energy, a clean energy carrier from a sustainable source of energy, Int. J. Energy Res. 44 (6) (2020) 4110–4131.
[207] C. Wulf, J. Linßen, P. Zapp, Review of power-to-gas projects in Europe, Energy Procedia 155 (2018) 367–378.
[208] A. Fernández-Guillamón, K. Das, N.A. Cutululis, A. Molina-García, Offshore wind power integration into future power systems: Overview and trends, J. Mar. Sci. Eng. 7 (11) (2019) 399.
[209] J.C. Koj, C. Wulf, P. Zapp, Environmental impacts of power-to-X systems-A review of technological and methodological choices in Life Cycle Assessments, Renew. Sustain. Energy Rev. 112 (2019) 865–879.
[210] C. Schnuelle, J. Thoeming, T. Wassermann, P. Thier, A. von Gleich, S. Goessling-Reisemann, Socio-technical-economic assessment of power-to-X: Potentials and limitations for an integration into the German energy system, Energy Res. Soc. Sci. 51 (2019) 187–197.
[211] K. Dehghanpour, S. Afsharnia, Electrical demand side contribution to frequency control in power systems: a review on technical aspects, Renew. Sustain. Energy Rev. 41 (2015) 1267–1276, http://dx.doi.org/10.1016/j.rser.2014.09.015.
[212] V. Lakshmanan, M. Marinelli, J. Hu, H.W. Bindner, Provision of secondary frequency control via demand response activation on thermostatically controlled loads: Solutions and experiences from Denmark, Appl. Energy 173 (2016) 470–480, http://dx.doi.org/10.1016/j.apenergy.2016.04.054.
[213] S.A. Hosseini, M. Toulabi, A. Ashouri-Zadeh, A.M. Ranjbar, Battery energy storage systems and demand response applied to power system frequency control, Int. J. Electr. Power Energy Syst. 136 (2022) 107680, http://dx.doi.org/10.1016/j.ijepes.2021.107680.
[214] A. Al-Hinai, H. Alyammahi, H. Haes Alhelou, Coordinated intelligent frequency control incorporating battery energy storage system, minimum variable contribution of demand response, and variable load damping coefficient in isolated power systems, Energy Rep. 7 (2021) 8030–8041, http://dx.doi.org/10.1016/j.egyr.2021.07.072.
[215] A. Malik, J. Ravishankar, A hybrid control approach for regulating frequency through demand response, Appl. Energy 210 (2018) 1347–1362, http://dx.doi.org/10.1016/j.apenergy.2017.08.160.

[216] H. Liu, J. Qi, J. Wang, P. Li, C. Li, H. Wei, EV dispatch control for supplementary frequency regulation considering the expectation of EV owners, IEEE Trans. Smart Grid 9 (4) (2018) 3763–3772, http://dx.doi.org/10.1109/TSG.2016.2641481.

[217] J. Zhong, L. He, C. Li, Y. Cao, J. Wang, B. Fang, L. Zeng, G. Xiao, Coordinated control for large-scale EV charging facilities and energy storage devices participating in frequency regulation, Appl. Energy 123 (2014) 253–262, http://dx.doi.org/10.1016/j.apenergy.2014.02.074.

[218] H. Jia, X. Li, Y. Mu, C. Xu, Y. Jiang, X. Yu, J. Wu, C. Dong, Coordinated control for EV aggregators and power plants in frequency regulation considering time-varying delays, Appl. Energy 210 (2018) 1363–1376, http://dx.doi.org/10.1016/j.apenergy.2017.05.174.

[219] J. Hu, J. Cao, L. Rutkowski, C. Xue, J. Yu, Hierarchical interactive demand response power profile tracking optimization and control of multiple EV aggregators, Electr. Power Syst. Res. 208 (2022) 107894, http://dx.doi.org/10.1016/j.epsr.2022.107894.